FIRE MODELLING STANDARDS/BENCHMARK

Report on Phase 1 Simulations

by

A.J.Grandison, E.R.Galea and M.K.Patel

Fire Safety Engineering Group.
University of Greenwich
London SE10 9LS.

for

Dr David Peace
Head
Fire Research And Development Group.
Home Office.

FEBURARY 2001.

Contents

EXECUTIVE SUMMARY

The purpose of the proposed standards/benchmarks is to aid the fire safety approvals authority in assessing the appropriateness of using a particular model for a particular fire modelling application. This benchmark has been split into two phases. The first phase is intended to test all the software products using identical or equivalent models. The second phase of testing allows the full range of the software's capability to be demonstrated. In each phase, five non-fire (CFD) and five fire cases are tested.

The first phase of the testing programme has been successfully completed. In studying the outcome of the Phase 1 test cases, it is clear that when identical physics is activated, identical computational meshes used and similar convergence criteria applied, all of the software products (PHOENICS, CFX and SMARTFIRE) tested are capable of generating similar results. This is an important observation and suggests – within the limitations of the tests undertaken – that these three codes have a similar basic capability and are capable of achieving a similar basic standard. While there are minor differences between the results generated by each of the software products; on the whole they produce – for practical engineering considerations – identical results. From a regulatory viewpoint, it is reassuring to have an independent verification of this similarity.

The one area that showed relatively poor agreement between model predictions and theoretical results concerned the six-flux radiation model performance. The six-flux radiation model while capable of representing the average trends within the compartment, does not produce an accurate representation of local conditions.

CFX, PHOENICS and SMARTFIRE all provide alternative radiation models which may offer superior performance. This has been demonstrated for the CFX 12-ray Shah-Lockwood model within this document. It should be noted that the six-flux model was used as it was common to both PHOENICS and SMARTFIRE, and CFX could be made to crudely approximate the six-flux model. However, CFX does not possess a six-flux model and so the Shah-Lockwood model was used with a single ray to give the closest approximation possible to the six-flux model. It should be noted that the developers of CFX generally advises that the CFX radiation model should never be used with a single ray. As mentioned previously the intention of phase-1 was to test the codes in as similar a manner as possible to try and give an unbiased reflection of how the codes compared. This task would not have been possible unless the CFX single ray radiation model was used.

A significant – and somewhat reassuring - conclusion to draw from these results is that an engineer using the basic capabilities of any of the three software products tested would be likely to draw the same conclusions from the results generated irrespective of which product was used. From a regulators view, this is an important result as it suggests that the quality of the predictions produced are likely to be independent of the tool used – at least in situations where the basic capabilities of the software are used.

A second significant conclusion is that within the limits of the test cases examined and taking into consideration experimental inconsistencies and errors, all three software products are capable of producing reasonable engineering approximations to the experimental data, both for the simple Computational Fluid Dynamics (CFD) cases (i.e. non-fire cases) and full fire cases.

An important element of this work concerned the procedures for undertaking the testing. While all of the test cases using all of the codes were run by a single organisation – in this case the Fire Safety Engineering Group (FSEG) at the University of Greenwich – the code developers also were requested to run an independent selection of the test cases as specified. This was necessary to verify that the results produced in this report are a true and fair representation of the capabilities of the various software products under the specified test conditions. This has proven to be quite useful as it brings the developers into the benchmarking process and it eliminates issues concerning fairness and biased reporting of results.

What remains to be completed at this stage are the Phase 2 results produced by the other testers. In Phase 2, the modellers are free to select which of the test cases to repeat using the full capability of their software to give the best possible representation of the case. These results will then be checked by FSEG for their veracity.

Finally, the concept of the Phase 1 testing protocols has been shown to be a valuable tool in providing a verifiable method of benchmarking and gauging the basic capabilities of CFD based fire models on a level playing field. To further improve the capabilities of the approach, it is recommended that additional test cases in the two categories (basic CFD non-fire and fire) be developed.

1.0 Introduction

The Fire Modelling Standards/Benchmark (FMSB) project marks the first step in the development of a set of standards/benchmarks that can be applied to fire field models. The project is led by the University of Greenwich's Fire Safety Engineering Group (FSEG) and funded by the Home Office Fire Research and Development Group. It is not the intent of the current stage of this project to define definitely the entire range of standards/benchmarks but to suggest and demonstrate the principle behind the proposed standards and to propose the required next steps. It is expected that the suite of cases will evolve over time as suitable new experimental data are made available or as new theoretical cases are developed.

The ultimate purpose of the proposed standards/benchmarks is to aid the fire safety approvals authority e.g. fire brigade, local government authority, etc in assessing the appropriateness of using a particular model for a particular application. Currently there is no objective procedure that assists an approval authority in making such a judgement. The approval authority must simply rely on the reputation of the organisation seeking approval and the reputation of the software being used. In discussing this issue it must be clear that while these efforts are aimed at assisting the approval authorities, there are in fact three groups that are involved, the approvals authority, the general user population and the model developers. Ideally, the proposed standards/benchmark should be of benefit to all three groups. In proposing the standards/benchmark, it is not intended that meeting these requirements should be considered a SUFFICIENT condition in the acceptance process, but rather a NECESSARY condition. Finally, the benchmarks are aimed at questions associated with the software, not the user of the software.

This document marks the conclusion of the first phase of the project, the performance of the phase 1 simulations. The broad definition of the Phase 1 and Phase 2 simulations may be found in section 2.3 with the precise definition of the phase 1 problems for each of the software products being defined in Appendix B and C. Results for the phase 1 simulations are presented along with a discussion of the results.

2.0 Background

It is essential to set standards/benchmarks to assess both the Computational Fluid Dynamics (CFD) engine and the fire model component for each type of code. However, within the fire modelling community, testing of fire field models has usually completely ignored the underlying CFD engine and focussed on the fire model. Thus, when numerical fire predictions fail to provide good agreement with the benchmark standard, it is not certain if this is due to some underlying weakness in the basic CFD engine, the fire model or the manner in which the problem was set-up (i.e. questions of user expertise). Furthermore, the case that is being used as the benchmark/standard is usually overly complex or cannot be specified to the precise requirements of the modellers. All of this is often to the benefit of the code developer/user as it allows for a multitude of reasons (some may say excuses) to explain questionable agreement.

Furthermore, what fire modelling testing that is undertaken is usually done in a non-systematic manner, performed by a single individual or group and is generally based around a single model. Thus it is not generally possible for other interested parties to exactly reproduce the presented results (i.e. verify the results) or to apply the same protocol to other models. This makes verification of the results very difficult if not impossible and the comparison of one model with another virtually impossible.

When discussing standards/benchmarks, there are essentially three groups of interested party, the approval authorities, the user groups and the software developer. While maintaining the highest level of safety standards is of general interest to all parties, each interest group has a specific reason for requiring a standard/benchmark. In order to maintain safety standards, the approvals authority must be satisfied that appropriate tools have been employed, the user wants to be assured that he is investing in technology that is suited to the intended task, while the developer would like to have a definable minimum target to achieve.

To satisfy the differing requirements of the approvals authority, user and software developer populations, any suite of benchmarks/standards must be both diagnostic and discriminating. Hence, the proposed suite of benchmarks/standards would ideally exercise each of the components of the fire field model i.e. CFD engine and fire model. This means that standards based simply around instrumented room fire tests are insufficient. This would for example require benchmarks/standards for simple recirculating flows, buoyant flows, turbulent flows, radiative flows, etc. Furthermore, in addition to the quality of the numerical results, details of the computer and compiler used to perform the simulations and the associated CPU time expended in performing the calculations could be provided. While not of particular interest to the approval authorities, this will be of interest to the user community.

Ideally, the proposed benchmarks/standards will evolve into a measure of quality, indicating that the fire model has reached a minimum standard of performance. This does not necessarily mean that the software may be used for any fire application, however it would eliminate from consideration those software products that have not demonstrated that they can attain the standard.

2.1 THE SOFTWARE PRODUCTS (SP)

Several developers of well known fire field models currently used in the UK were approached to participate in this project namely, the developers of JASMINE, SOFIE, CFX, PHOENICS and SMARTFIRE. Three code developers agreed to participate in this first phase. These are:

The general purpose CFD codes,
CFX 4.2 [1] and
PHOENICS 3.1 [2]

and the specific fire field model,
SMARTFIRE v2.01 b389D[3].

These versions of the code were the latest available versions of the code at the University of Greenwich at the commencement of the project. Originally PHOENICS 2.1.3 was used but was changed to 3.1 for reasons described in Appendix A.

2.2 BENCHMARK TASK GROUP

Representatives from the organisations responsible for the identified software products (SP) constitute the Benchmark Task Group (BTG). In addition, the BTG consists of one independent user of fire field models drawn from the user community (Arup Fire) and a representative from the FRDG. The role of the BTG is to review the proposed benchmarks and specified solution procedures and to review the final results. The BTG is chaired by Prof. Ed Galea of FSEG.

2.3 BENCHMARK PROCEDURES

The benchmarks are divided into two categories, basic CFD and fire. Two types of simulation are to be performed by each SP being subjected to the benchmarks; these are to be known as phase 1 and phase 2 simulations. The nature of the phase 1 simulation has been rigidly defined by FSEG under review by the BTG, this includes the mesh specification, physics to be activated, algorithms to be employed and results to be generated (see Appendix B and C). Where possible, the specification of phase 1 simulations has been such that all of the SP participating in the trial will be able to achieve the specification. It is acknowledged that this process will not necessarily produce optimal results for all of the SPs.

The phase 1 simulations will be completed before proceeding to attempt the phase 2 simulations. The phase 2 simulations will be free format in nature, allowing the participants to repeat the simulation using whatever specification they desire. Phase 2 simulations will allow the participants to demonstrate the full capabilities of their SP. However, phase 2 simulations will only be allowed to utilise features that are available within their software product i.e. additional code or external routines are not permitted.

Each phase 1 simulation will be performed at least once. FSEG will run each phase 1 simulation with each SP. The participants are requested to run at least two of the 10 phase 1 simulations using their SP. Participants are free to choose which of two simulations to run, however these must include at least one from the CFD category and one from the fire category. Participants are of course free to (and indeed encouraged to) run all 10 of the phase 1 simulations. It is however imperative that the participants do not inform FSEG which of the phase 1 simulation they intend to run. It should be remembered that the purpose of repeating the simulations is to ensure that FSEG have not fabricated results.

On completing the phase 1 simulations participants will be invited to undertake their phase 2 simulations. All participants must complete a similar pro-forma that has been supplied for the phase 1 simulations. This is necessary as FSEG will repeat the phase 2 simulations in order to independently verify the results.

2.4 THE BENCHMARK CASES

As a first attempt at defining the benchmarks, 10 cases are considered, these involve five CFD cases and five fire cases. All of the phase 1 simulations are defined with relatively coarse meshes in order to keep computation times to reasonable levels. Participants are of course free to refine meshes when undertaking the phase 2 simulations. Complete specifications for these cases will soon be available on the FSEG web site.

The cases are defined as follows:

CFD Cases:
2000/1/1
Two dimensional turbulent flow over a backward facing step.
2000/1/2
Turbulent flow along a long duct.
2000/1/3
Symmetry boundary condition.
2000/1/4
Turbulent buoyancy flow in a cavity.
2000/1/5
Radiation in a three-dimensional cavity.

Fire Cases:
2000/2/1
Steckler Room (heat source).
2000/2/2
Steckler Room (combustion model).
2000/2/3
Fire in a completely open compartment with lid (heat source).
2000/2/4
CIB W14 fire (combustion model).
2000/2/5
Large fire (combustion model)

Full details concerning the specification of the phase 1 simulations may be found in Appendix B and C.

3.0 The Results

This section contains the results from the Phase-1 testing regime. Phase-2 testing results will be described in a future document.

The CFD and fire cases were designed to test the basic features of the SPs to ensure that these functioned correctly. In Phase-1, testing has been designed to ensure that the codes are set up as similarly as possible. This includes using the same computational mesh in all cases and the physics switched on in all cases consists of the lowest common denominator between the SPs. While this has been the aim of this part of the testing process, some differences may exist between the various SPs. The most obvious difference between the SPs is that PHOENICS uses a staggered velocity mesh whereas SMARTFIRE and CFX use a co-located velocity mesh by means of Rhie and Chow interpolation [4] and while SMARTFIRE and PHOENICS make use of a six-flux radiation model, CFX uses a more sophisticated model.

Some of the problems encountered on the project with the SPs are briefly highlighted in Appendix A.

Details of the numerical set-ups for the CFD and fire cases can be found in Appendix B and C.

3.1 CFD cases

In this section the results generated by FSEG for the CFD cases are presented. In the first four cases radiation either is not relevant to the situation or makes no significant contribution to the simulation and so is not modelled.

3.1.1 2000-1-1 – Backward Facing Step

This test is a standard CFD test case used by a number of CFD code developers. Its primary purpose is to test the turbulence model used by the CFD code. Results from the SPs are cross compared and predictions from the SPs are compared with experimental data. Comparative values have been taken at 0.285m downstream of the inlet and at the outlet. Predictions of the location of the stagnation point are compared with experimental data [5].

The flow is incompressible, fully turbulent and isothermal. The fluid has a density of 1.0 kg/m^3 and a laminar viscosity of 1.101E-5 kg/ms. The geometry of the case is illustrated in Figure 1.

The upper and lower surfaces are walls and there is a solid obstruction below the inlet. The fluid enters the chamber at 13.0 m/s.

See Appendix B.1 for further setup details.

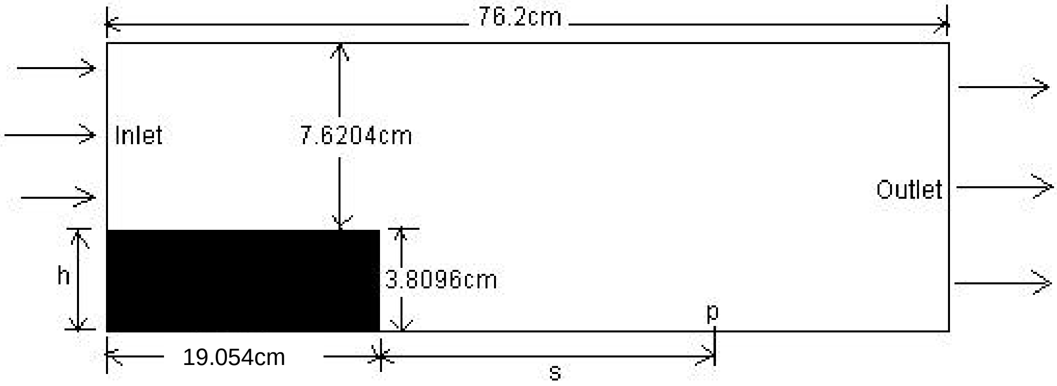

Figure 1 - Backward facing step configuration

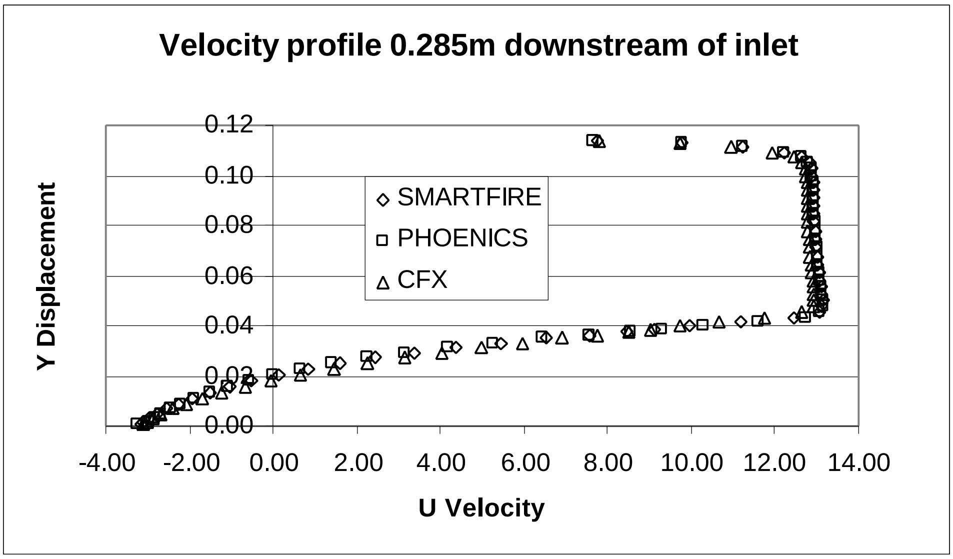

Figure 2 - Velocity profile 0.285m downstream of inlet for 2000-1-1

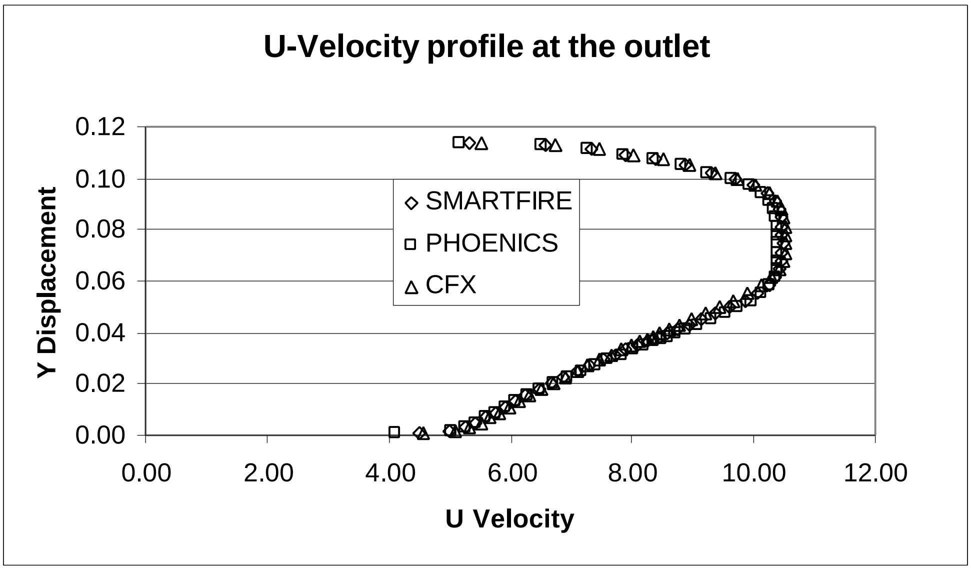

Figure 3 - Velocity profile at the outlet for 2000-1-1

In figures 2 and 3 it can be seen that there is extremely good agreement between the three SPs.

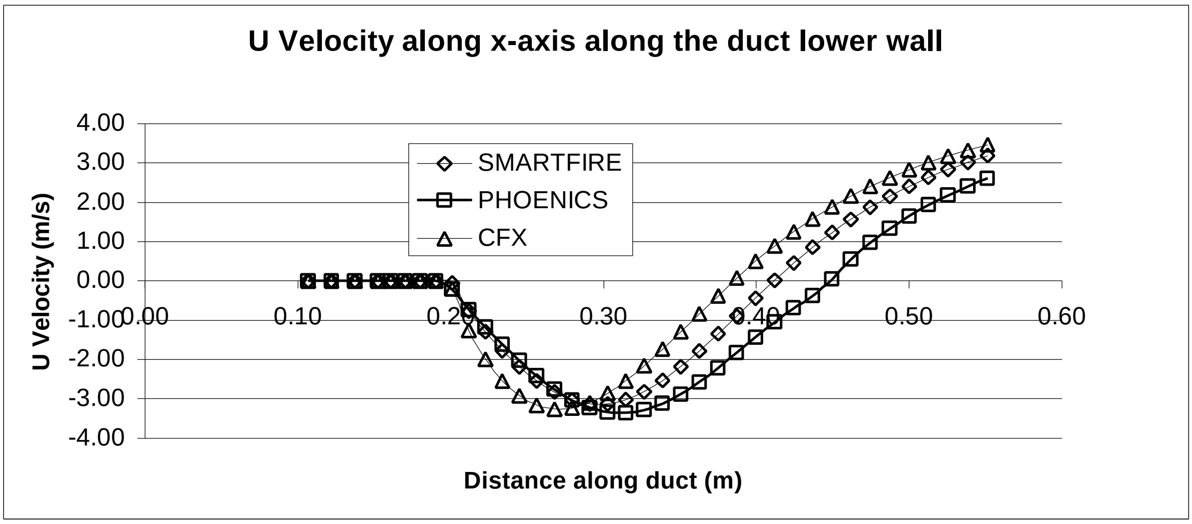

Figure 4 - U Velocity along the duct lower wall

Table 1 - Comparison of stagnation point for the CFD codes

Stagnation point	x	S	S/h (where h=.0381)
SMARTFIRE	0.412	0.2217	**5.82**
PHOENICS	0.449	0.2587	**6.79**
CFX	0.387	0.1967	**5.16**

The stagnation point is the point where the recirculation due to the step ends along the lower duct wall (point p in Figure 1). There is some variation in the predicted stagnation point ratio (S/h) (see Figure 4 and Table 1), the experimental value of 7.2 is most closely matched by PHOENICS followed by SMARTFIRE with CFX being the furthest away from the experimental value. However these values are obtained using each code's standard k-e turbulence model and improved results may be expected with enhanced turbulence models.

3.1.2 2000-1-2 Heat transfer in a long thin duct

This test is a standard CFD test case used by a number of CFD code developers. Its primary purpose is to test the turbulence model in conjunction with turbulent heat transfer. Predictions of the velocity and enthalpy profile at the outlet are cross compared.

The geometry of the case is depicted in Figure 5. The flow is non-buoyant, fully turbulent, incompressible with heat transfer but with no radiation. Flow enters the inlet at 50m/s with an enthalpy of 50 J/Kg. The wall has a fixed enthalpy value of 1 J/Kg. The fluid density is 1.0 kg/m^3, the conductivity is 0.07179 W/mK, the density is 1.0 kg/m^3, laminar viscosity is 5e-5 kg/ms, specific heat is 1005 J/kgK

See Appendix B.2 for further setup details.

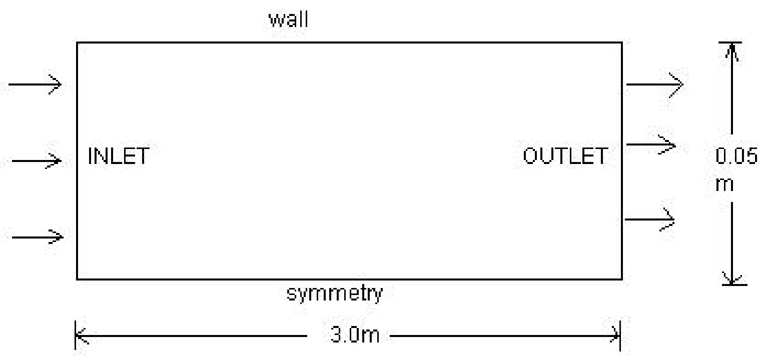

Figure 5 - Turbulent long duct flow configuration

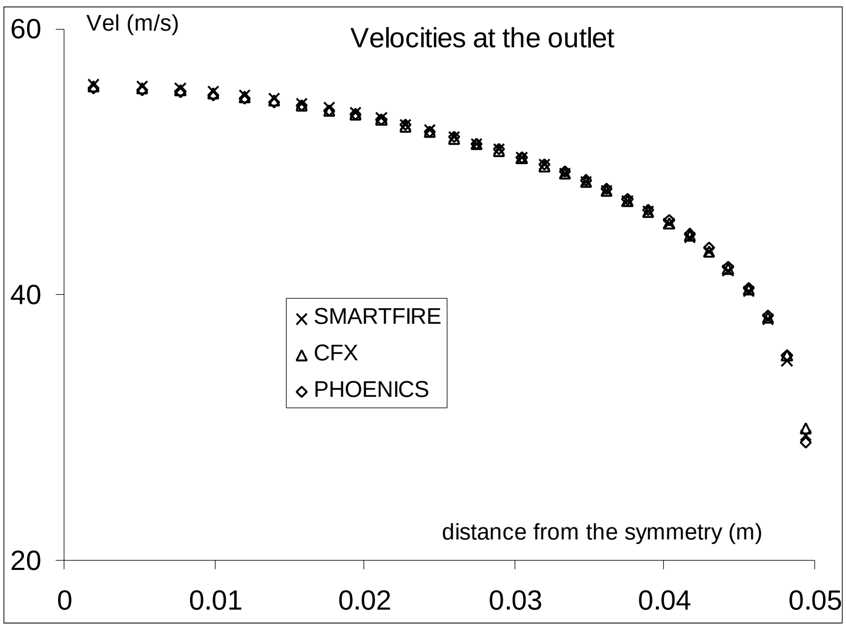

Figure 6 - Velocity profile at outlet for 2000-1-2

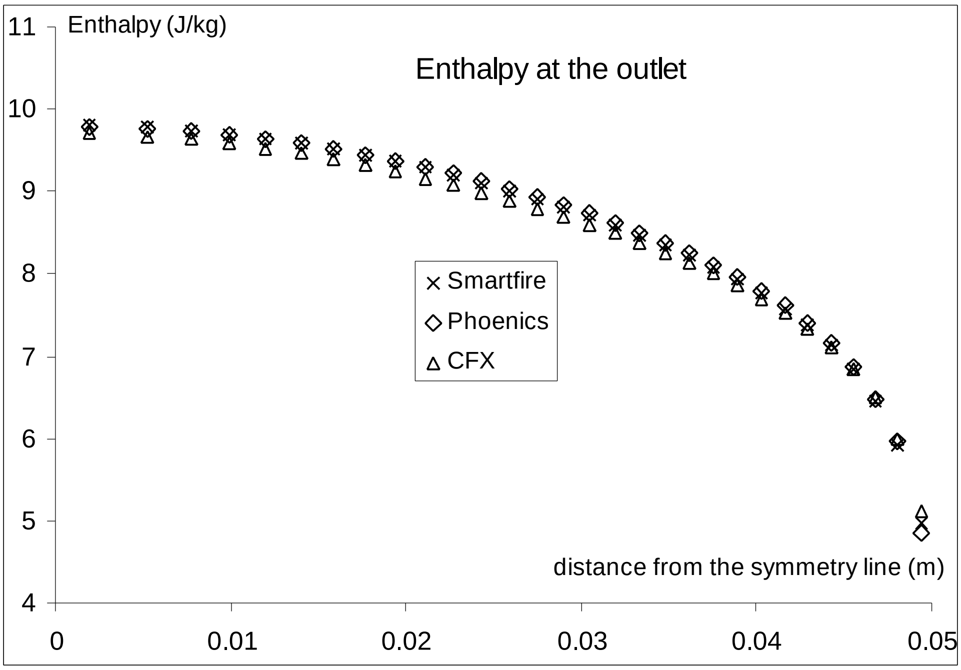

Figure 7 - Enthalpy profile at the outlet for 2000-1-2

Depicted in Figure 6 is the velocity profile generated by the three SPs at the outlet, while depicted in Figure 7 is the enthalpy profile at the outlet. As can be seen from these figures, there is extremely good agreement across the SPs.

3.1.3 2000-1-3 Symmetry

This test is a relatively simple CFD test case. Its primary purpose is to test if the symmetry function works correctly for turbulent isothermal flow situations. Model predictions for the symmetric case are compared with and without the symmetry function in operation. The predictions from the SPs are also cross compared.

The case involves flow expansion from a small duct into a larger duct. The configuration is shown in Figure 8 below. The case was simulated using the whole flow domain and then repeated using a symmetry boundary condition along the central axis. Two tests must be conducted using the full domain and using a half domain with a symmetry plane. The results from these two tests should agree with one another. The flow enters the domain at 1.0m/s.

See Appendix B.3 for further setup details.

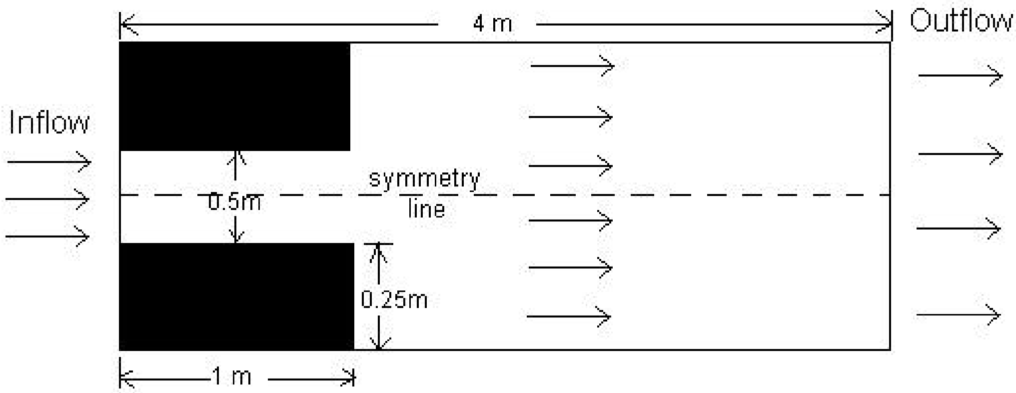

Figure 8 - Expanding duct with symmetry line indicated

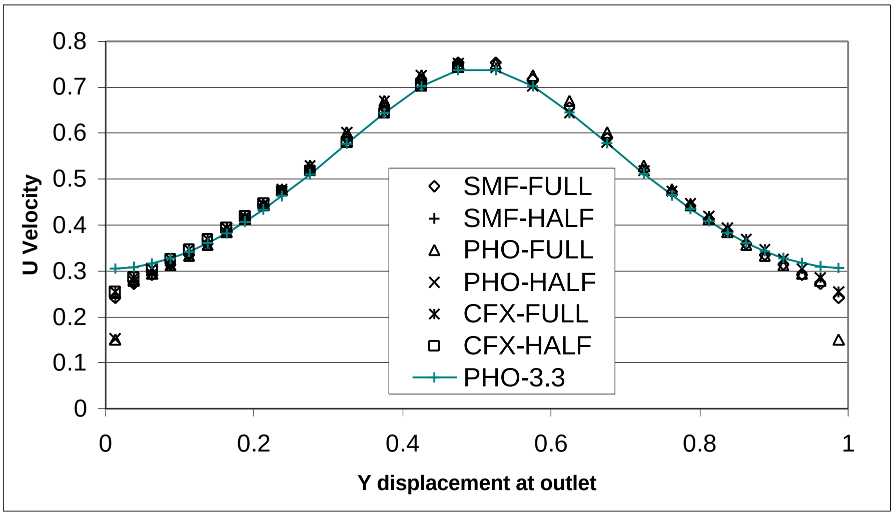

Figure 9 - U Velocity profile at the outlet for 2000-1-3

All the U-velocity profiles for all the codes using both the full and half geometry are encapsulated in Figure 9. Within the SPs the same results for the U velocity at the outlet have been produced for the symmetry (half) and full geometry versions of the test case. Across the codes the results were also close to one another although the PHOENICS generated nearest wall velocity is significantly different to that of SMARTFIRE and CFX. CHAM – the developers of PHOENICS – repeated the above test case using a more recent version of PHOENICS, i.e. PHOENICS V3.3 and found that the velocity at the wall was increased compared to the result generated using V3.1. The result is now slightly faster than that produced by CFX and SMARTFIRE but is more inline with the general trends. FSEG has verified these results.

3.1.4 2000-1-4 Buoyant turbulent flow

This test is a standard CFD test case used by a number of CFD code developers. Its primary purpose is to test the turbulence model, turbulent heat transfer and buoyancy model. Predictions of a number of parameters are made and cross compared. Model predictions are also compared with experimental results [6].

The geometry used for this case is depicted in Figure 10 below.

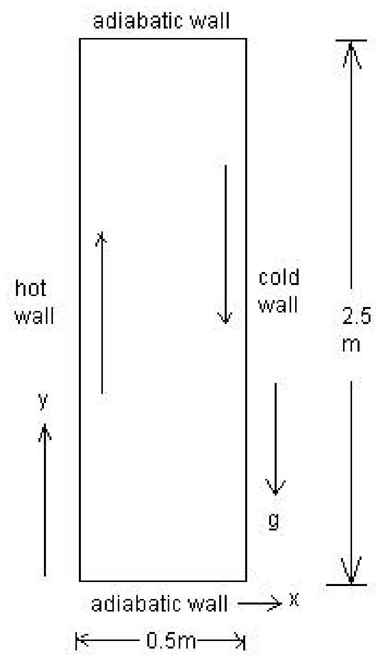

Figure 10 – Configuration for buoyancy flow in a duct

The flow is fully turbulent, buoyant and fully compressible but with no radiative heat transfer. The hot wall is at a temperature of 353K and the cold wall is at 307.2K. The other walls are adiabatic. The acceleration due to gravity (g) is –9.81m/s^2. The fluid has the following properties:

conductivity is 2.852158e-02 (W/mK)
density is 1.071 (kg/m^3) determined by ideal gas law as fully compressible.
specific heat is 1.008e+03 (J/kgK)
laminar viscosity is 2.0383e-05 (kg/ms)
thermal expansion is 3.029385e-03 (1/K).

See Appendix B.4 for further setup details.

Model predictions are presented for the following:

The v-velocity profile at y/H = 0.5
The normalised temperature profile at y/H = 0.5 and x/L = 0.5

where $T_{normalised} = (T_{actual} - T_{cold})/(T_{hot} - T_{cold})$
The turbulent fluctuations, $\sqrt{k}$, at y/H = 0.5
The turbulent viscosity scaled with the laminar viscosity at y/H = 0.5.

In the above, L is full length across the x direction of the duct (0.5m) and H is the full height of the duct in the y direction (2.5m).

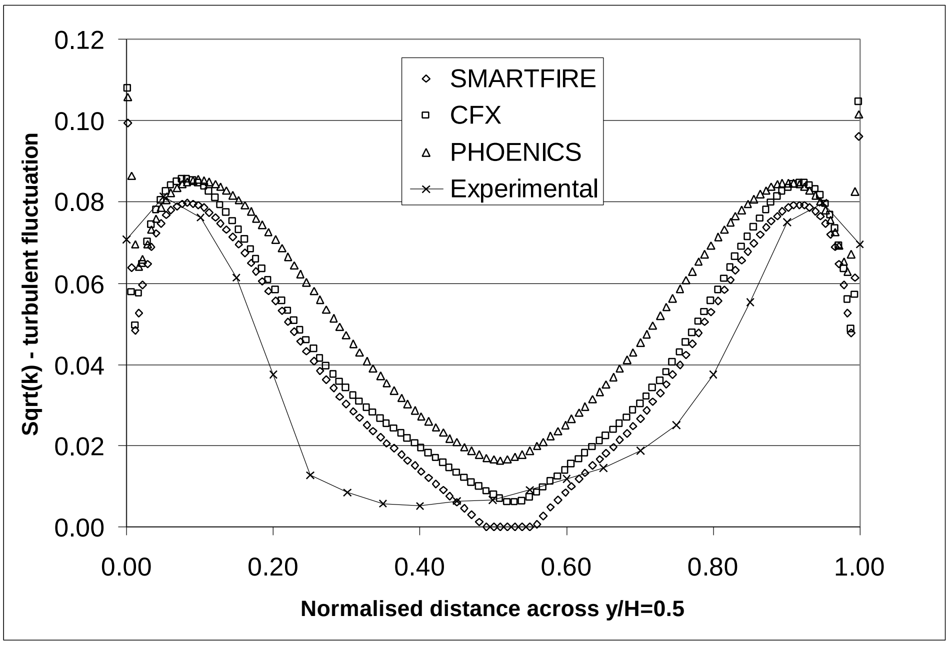

Figure 11 - Turbulent fluctuations across y/H=0.5 for 2000-1-4

Depicted in Figure 11 are the turbulent fluctuations at y/H=0.5 predicted by the SPs and the experimental results. All the codes are in reasonable agreement with one another although SMARTFIRE has a noticeable point where no turbulent fluctuations exist. All the SPs results are in good agreement with the experimental data. All the models exhibit high values close to the walls that are not reflected in the experimental result, this is due to a shortcoming that exists in the standard high-Re k-ε model.

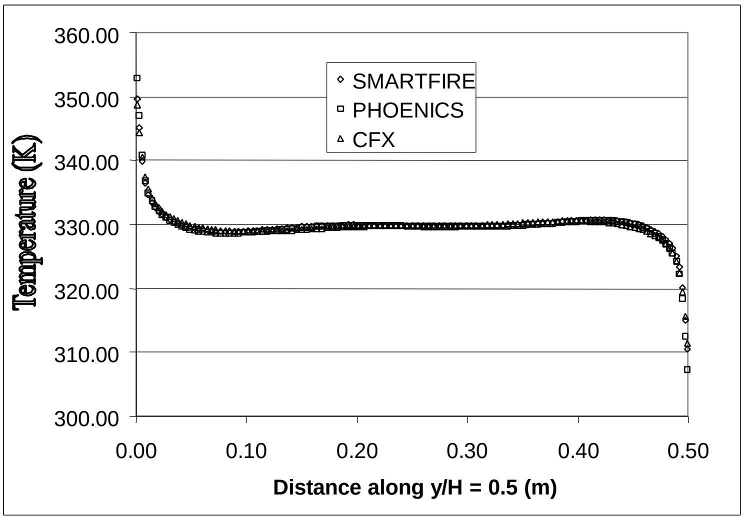

Figure 12 – Temperature variation along the y/H = 0.5 axis.

Depicted in Figure 12 are the temperature predictions along y/H = 0.5. As can be seen there is excellent agreement between the SP for the temperature variation across the x-axis.

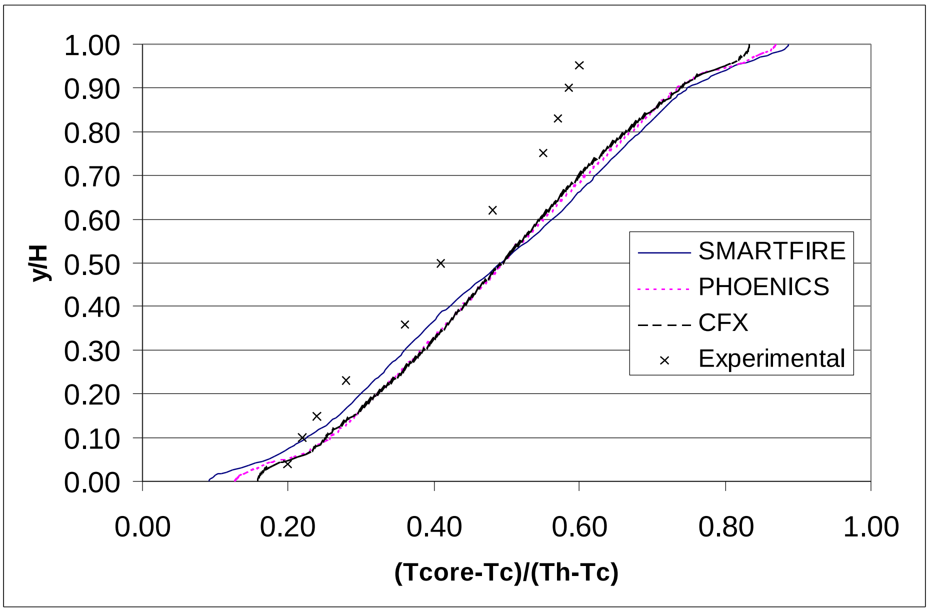

Figure 13 Temperature variation along the x/L = 0.5 axis

Depicted in Figure 13 are the temperature predictions along x/L = 0.5 predictions produced by the SPs and the experimental results. The SPs are in excellent agreement with each other although diverge from the experimental results at the higher end of the temperature differential. This difference is probably due to the three dimensional nature of the real problem and the heat losses which would occur on the top and bottom surfaces which have been assummed to be adiabatic in the modelling.

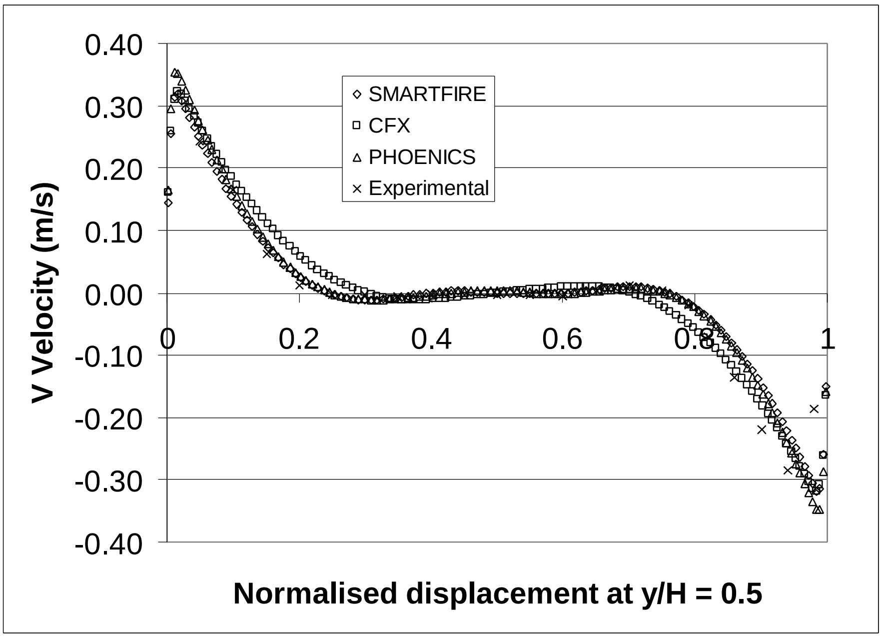

Figure 14 – Variation of V-Velocity along y/H = 0.5

Depicted in Figure 14 are the V velocity predictions and experimental results at y/H = 0.5. As can be seen, SMARTFIRE and PHOENICS are in reasonable agreement with one another. Both SPs produce slightly different results to CFX. It can be seen that the experimental values are closer to the SMARTFIRE and PHOENICS results between 0.0 – 0.5 and the experimental values are closer to CFX between 0.5 – 1.0.

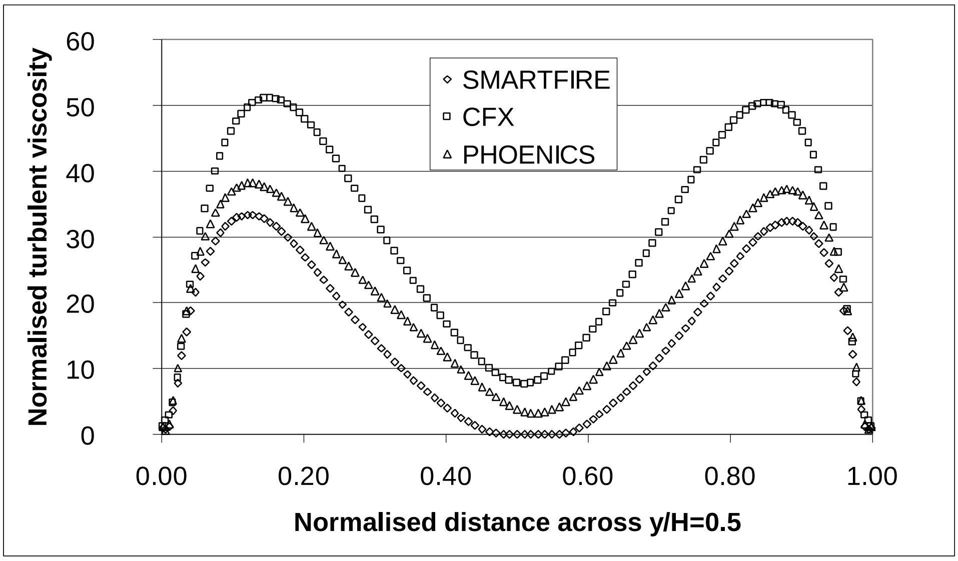

Figure 15 – Variation of normalised turbulent viscosity along y/H = 0.5.

Depicted in Figure 15 are the predictions for the normalised turbulent viscosity across y/H=0.5. As can be seen, SMARTFIRE and PHOENICS predictions are in reasonable agreement with each other while CFX predicts a far greater turbulent viscosity. There are no experimental results for this parameter and so it is difficult to conclude which set of predictions are correct. Also note that SMARTFIRE predicts that the normalised turbulent viscosity goes to zero at the centre.

From Figure 11 to Figure 14 it can be seen that there is reasonable agreement between the codes and experimental data. While some differences exist between the codes, these are not considered to be significant.

3.1.5 2000-1-5 Radiation in a 3D cavity.

The primary purpose of this test case was to test the radiation model used by the SPs. Model predictions are cross compared and also compared with theoretical predictions derived from detailed zone methods.

The geometry used for this test case consists of a three dimensional unit cube (1m x 1m x 1m) cavity with three walls with planes x=1, y=0 and z =0 set to a unit emissive power and the three other walls set to zero emissive power. All the walls are considered radiatively black have unit emissivity and the fluid has a unit absorption coefficient. Scattering is neglected. No fluid flow is considered

For the CFX cases it was not possible to generate a radiation grid with the same number of cells as CFD cells. In order to generate an approximately equivalent model to that of SMARTFIRE and PHOENICS a CFD grid with 4 times as many cells in each of the co-ordinate directions was generated. This allowed the creation of a radiation grid with the same number of cells as used by the other codes. This should produce approximately the same effect, as the radiation cells that contain the medium will have the same temperature as the CFD cells as energy is only transported radiatively. This is seen in the stepped profiles from the CFX cases. The CFX cases were run in two configurations, the first using a single ray to emulate the behaviour of the six flux models of SMARTFIRE and PHOENICS, and using 12 rays which is the default option for the CFX radiation model.

See Appendix B.5 for further setup details.

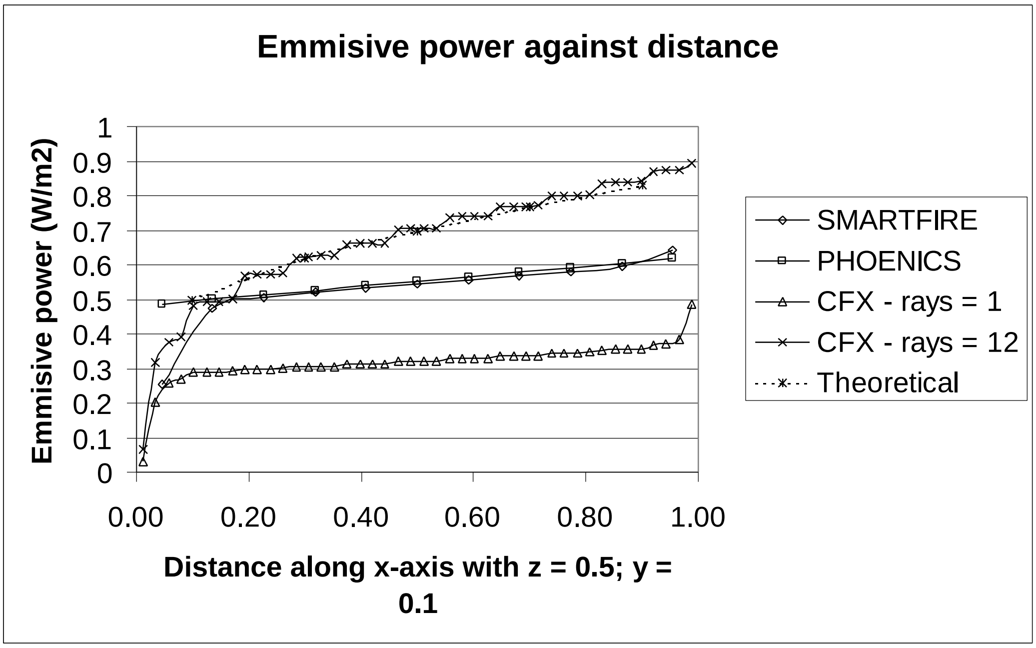

Figure 16 - Emissive power against distance along x-axis for z = 0.5; y = 0.1

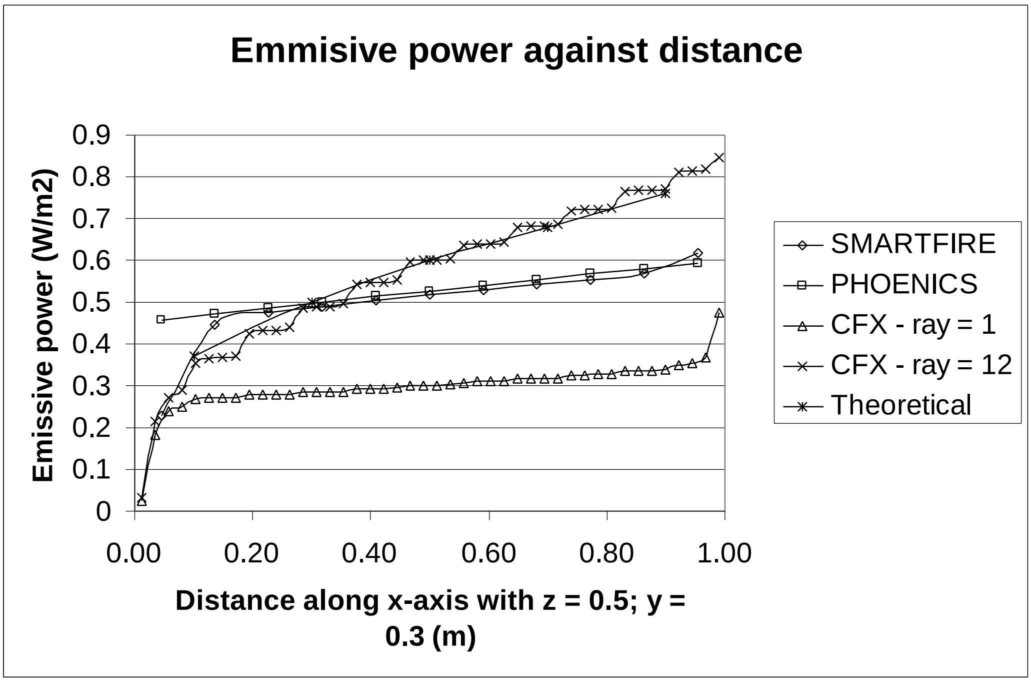

Figure 17 - Emissive power against distance along x-axis for z = 0.5; y = 0.3

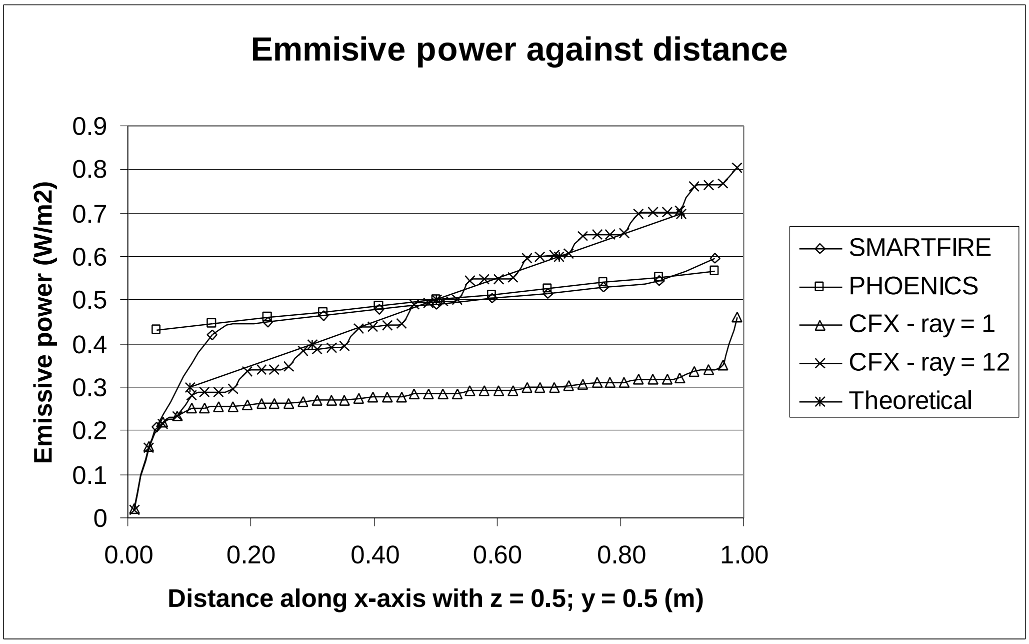

Figure 18 - Emissive power against distance along x-axis with z = 0.5; y = 0.5

In the above figures (Figure 16, Figure 17 and Figure 18) it can be seen that the 12-ray CFX radiation model produces a very good approximation to the theoretical emissive power. The six-flux model used by PHOENICS and SMARTFIRE – while producing similar results - only provides a crude approximation to the theoretical emissive power.

It should be noted that the one-ray CFX radiation model is not mathematically equivalent to the six-flux model, because of the manner in which direction is discretised. In fact, as the results demonstrate, it is cruder than the six-flux model. Users of the CFX code are generally advised not to use this radiation model with a single ray. The default setting for this model has 12 rays specified._The difference between the 12 ray model and the six flux model is not surprising as the resolution of the radiation field is expected to be much better when using 12 rays as opposed to one ray. Furthermore, the six-flux model relies on a high degree of scattering to distribute the radiation and no scattering is present in this case. It should be further noted that the six-flux model is not intended for applications where the accuracy of the heat flux at a solid surface is a crucial component of the calculations, such as situations involving flame spread over solid surfaces or when structural interaction with the fire is being predicted. It is intended for applications where the dominant factor is the radiative heat loss from the flame. This is commonly the situation when representing non-spreading fires.

3.2 Fire cases

In this section the results generated by FSEG for the fire cases are presented.

3.2.1 2000-2-1 & 2000-2-2 – Steckler fire case

This test is a standard fire model test case used by a number of field and zone model developers. Its primary purpose is to test the fire models predictive capability in predicting temperature and flow distributions in a small compartment subjected to a steady non-spreading fire. Predictions of several parameters are made and cross compared. Model predictions are also compared with experimental results [7].

The non-spreading fire was created using a centrally located (position A in Figure 19) 62.9kW methane burner with a diameter of 0.3m. The experiments were conducted by Steckler et al. in a compartment measuring 2.8m × 2.8m in plane and 2.18m in height (see Figure 19) with a doorway centrally located in one of the walls measuring 0.74m wide by 1.83m high. The walls and ceiling were 0.1m thick and they were covered with a ceramic fibre insulation board to establish near steady state conditions within 30 minutes.

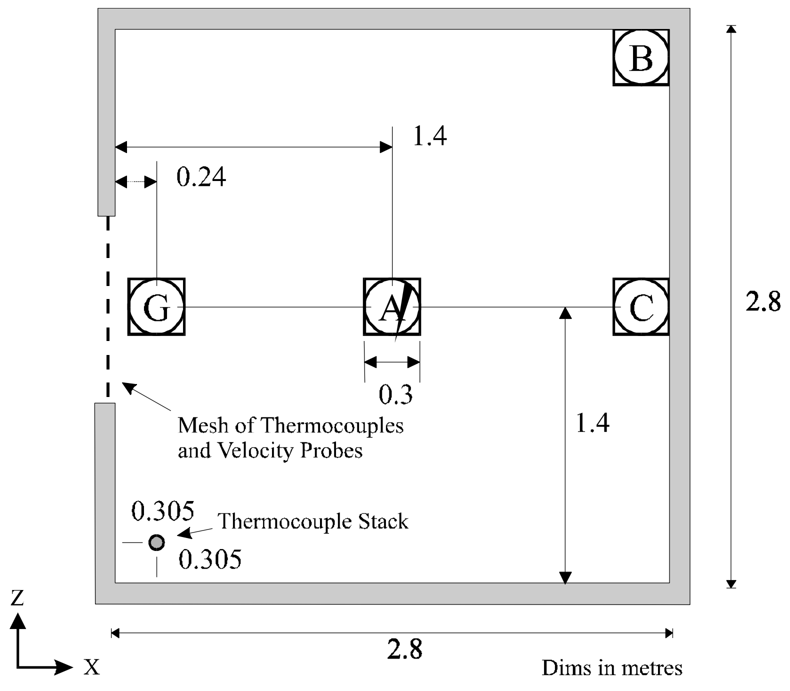

Figure 19 – Configuration of Steckler room

The door measures 0.74m wide and 1.83m high and is centrally located in one of the walls. Within the models, the walls are all assumed to be adiabatic and perfect radiative reflectors. The case is run for 200s of simulated time using 200 timesteps of 1s at which point steady state conditions are achieved in the simulation.

This case has been modelled using 2 methods: -
1) Using a simple volumetric heat source (2000-2-1)
2) Using a combustion model (2000-2-2)

In PHOENICS and SMARTFIRE a six-flux radiation model is used, while in CFX the discrete transfer model is used with a single ray in the co-ordinate direction to emulate the behaviour of a six-flux radiation model.

See Appendix C.1 and C.2 for further setup details.

Comparisons between the SPs using both a simple heat release model and a combustion model are presented below (Figure 20 - Figure 22). The comparison is made at two different locations; corner thermocouple stack located in one of the near corners to the doorway and a thermocouple and velocity measuring stack centrally located in the doorway (see Figure 19). The results presented are after 200s of simulated time at which point the results are steady state.

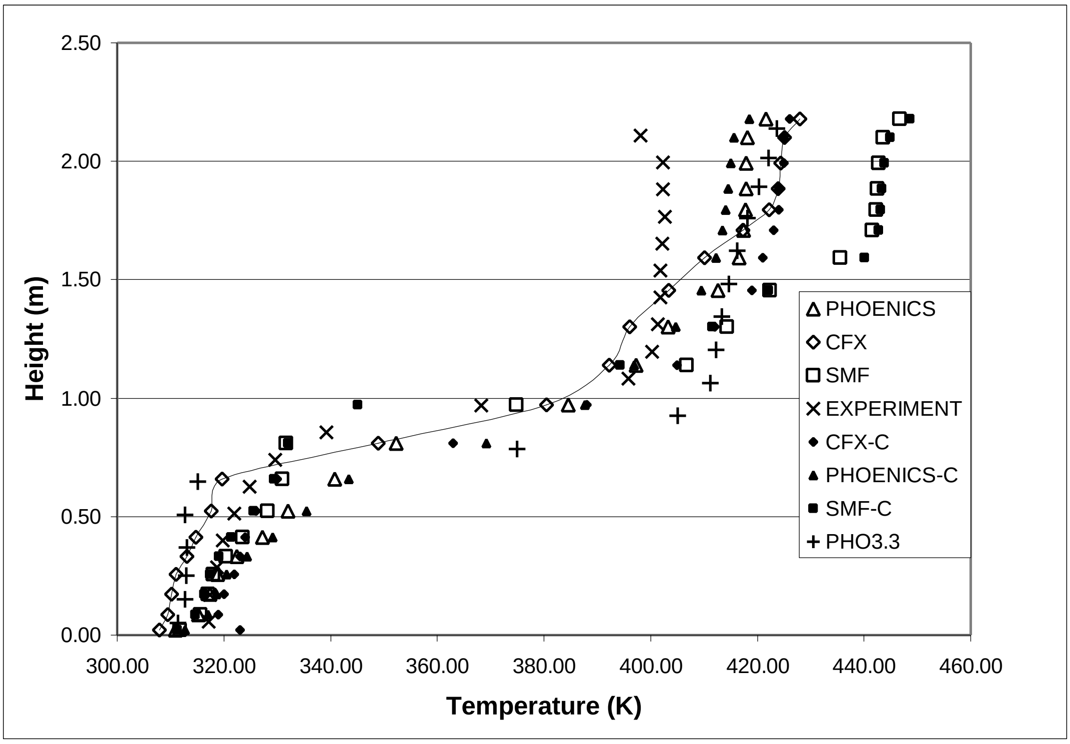

Figure 20 - Corner Stack temperatures produced using heat source model and combustion model.

Depicted in Figure 20 is the corner stack temperature profile generated by the SPs using the volumetric heat source model and the combustion model along with the experimental results. The temperature profile for the volumetric heat source model provided by CHAM using PHOENICS V3.3 is also supplied. It should be noted that FSEG did not attempt to repeat these calculations using V3.3 of PHOENICS and so there is no independent verification of these results. In viewing these results it must be remembered that the walls have been treated as adiabatic. As a result it is expected that the upper layer temperatures will be in excess of the measured temperatures.

Table 2 - Approximate upper heat layer temperature for Steckler's room (A74) using Heat Source model (H) and Combustion model (C).

	Exp	PHO-H	PHO-C	CFX-H	CFX-C	SMF-H	SMF-C	PHO3.3
Temp (K)	401	412	414	423	424	442	443	420

From Figure 20 and Table 2 it can be seen that all three SPs over predict the upper layer temperatures. It is interesting to note that the combustion models do not improve the prediction of the upper layer temperature. It is also interesting to note that all three SPs produce different estimates of the upper layer temperature, with SMARTFIRE predicting the hottest and furthest removed from the experimental value and PHOENICS predicting the coolest temperature and closest to the experimental value.

The location of the hot layer can be estimated by determining where uniform temperatures are established in the upper layer. From the experiment this appears to be at approximately 1.25m above the floor. Using PHOENICS the stratification layer appears to be about 1.5m above the floor with both the volumetric and heat source models. Using the volumetric heat source results provided by CHAM for PHOENICS V3.3 it was possible to estimate the height of the hot layer to be about 1.2m. Using the CFX heat source model the hot layer is approximately 1.75m above the floor while with the combustion model this becomes 1.5m. For SMARTFIRE, the hot layer is predicted to be at approximately 1.6m above the floor using either model.

Both CFX models capture the temperature trend below 1m reasonably well. Above the 1m the CFX heat source model does not capture the upper layer trend very well although the temperature predictions are not unreasonable given the adiabatic nature of the simulations compared to that of the experiment. The CFX combustion model produces a much better trend above 1m compared to the CFX heat source model.

Both SMARTFIRE models produce very similar results to one another. The trend below 1m is well captured although above 1m the temperature is hotter than the experiment and that predicted by both PHOENICS and CFX.

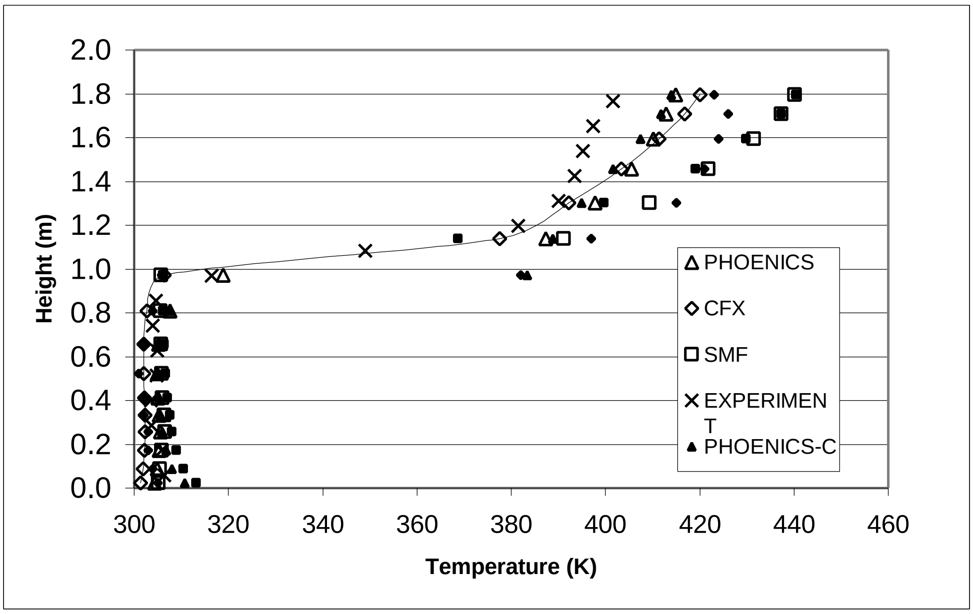

Figure 21 - Comparison of doorway temperatures for Steckler room

Depicted in Figure 21 is the doorway centre vertical temperature profile generated by the SPs using the volumetric heat source model and the combustion model along with the experimental results. In viewing these results it must be remembered that the walls have been treated as adiabatic. As a result it is expected that the upper layer temperatures and the resulting temperatures of the hot vented gases will be in excess of the measured temperatures.

From Figure 21 it can be seen that – as with the previous case - all three SPs over predict the temperature of the hot gases being vented out of the compartment. Once again, it is interesting to note that the combustion models do not improve the prediction of the hot vented gas temperature. It is also interesting to note that all three SPs produce different estimates of the vented hot gas temperature, with SMARTFIRE predicting the hotest and furtherest removed from the experimental value and PHOENICS predicting the coolest temperature and closest to the experimental value.

Depicted in Figure 22 is the doorway centre horizontal velocity profile generated by the SPs using the volumetric heat source model and the combustion model along with the experimental results. All the SPs appear capable of generating an excellent prediction of the velocity profile. Below the neutral plane SMARTFIRE and PHOENICS appear to best reproduce the velocity profile while above the neutral plane, high up in the door, PHOENICS appears to best reproduce the velocity profile.

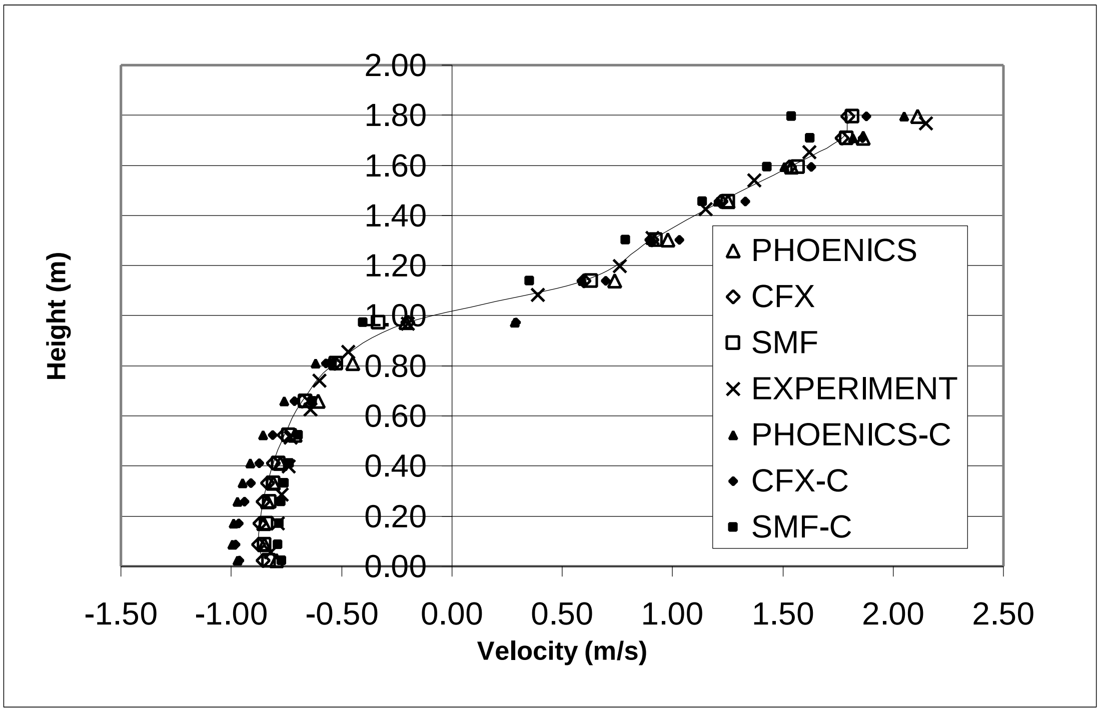

Figure 22 - Comparison of doorway velocity profiles for Steckler room

Depicted in Figure 23, Figure 24 and Figure 25 are temperature contour plots along the centre of the compartment for PHOENICS, CFX and SMARTFIRE respectively produced using the volumetric heat source model. From these temperature maps it can be seen that all the SPs produce similar trends. Most notable is the plume leaning away from the doorway. The temperature contours range from 320K to 500K and are separated by 20K increments. It can be seen that the lowest temperatures are produced by PHOENICS and the highest temperature is produced by SMARTFIRE, as would have been expected from the thermocouple stack comparisons (Figure 20 and Figure 21). The CFX and PHOENICS plume lean over by approximately the same amount with SMARTFIRE leaning over slightly less.

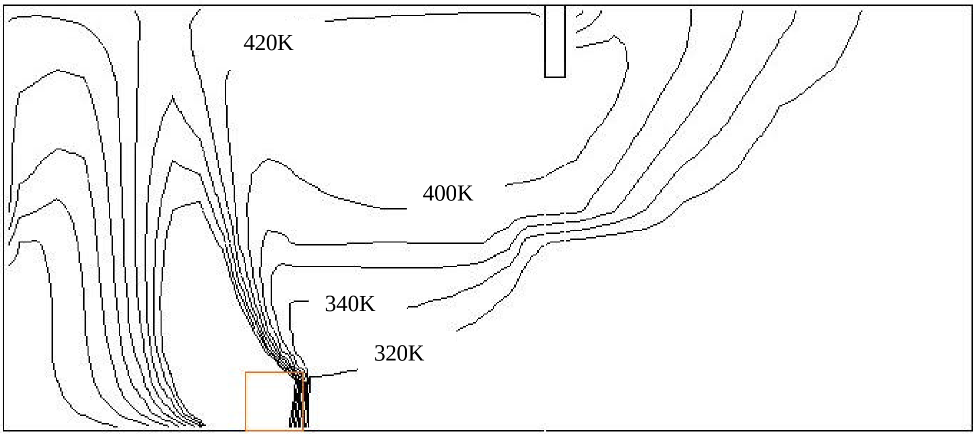

Figure 23 - Temperature contour plot produced by PHOENICS using the heat source model.

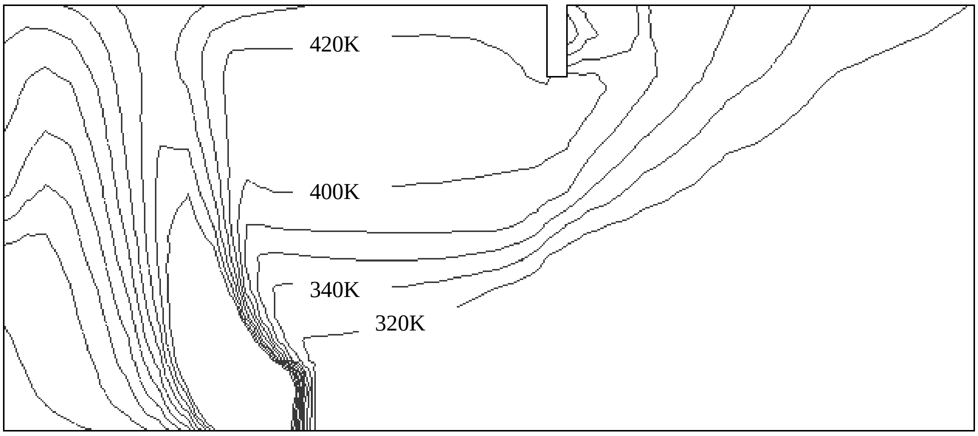

Figure 24 - Temperature contour plot produced by CFX using the heat source model.

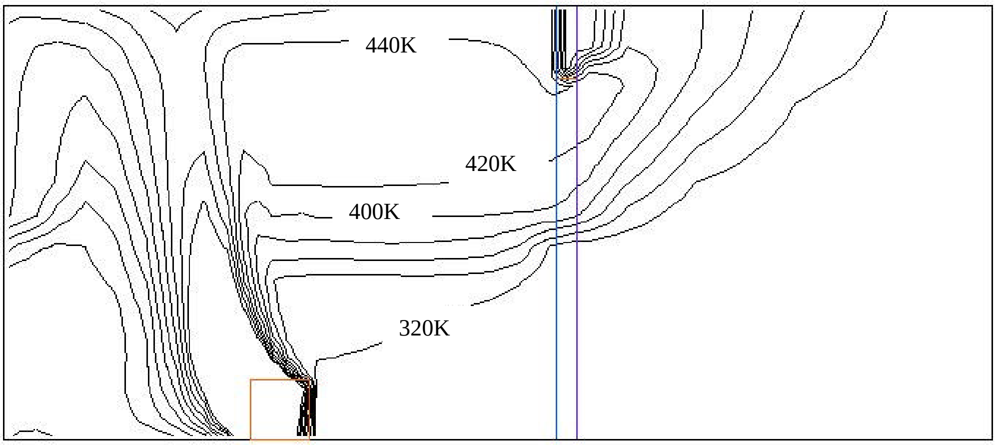

Figure 25 - Temperature contour plot produced by SMARTFIRE using the heat source model.

.

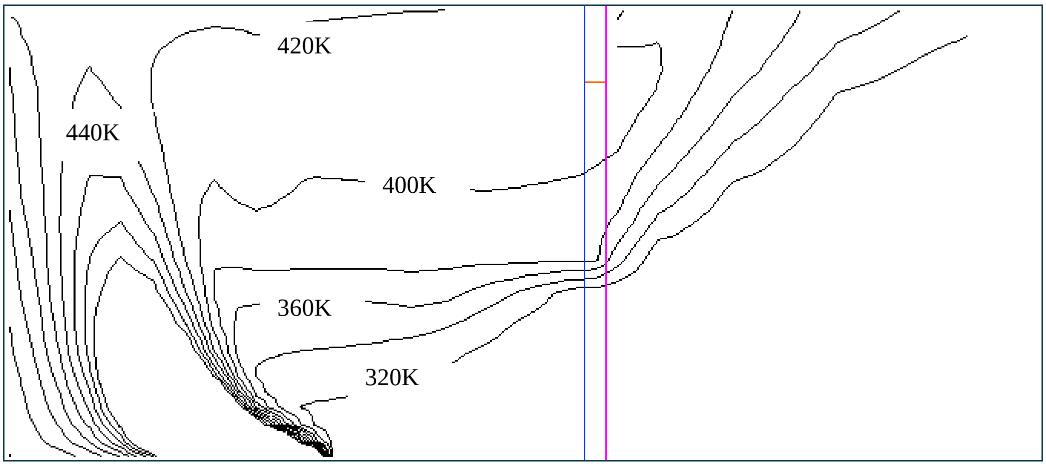

Figure 26 - Temperature contour plot produced by PHOENICS using the combustion model.

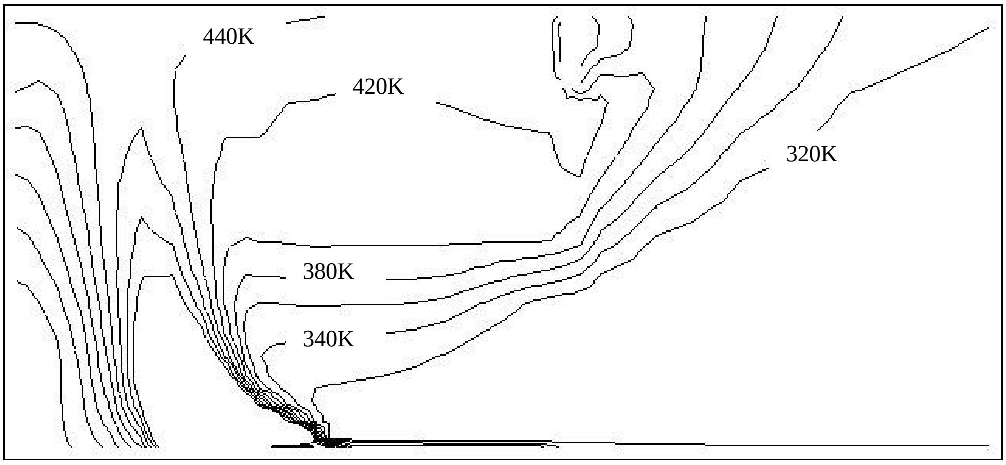

Figure 27 - Temperature contour plot produced by CFX using the combustion model.

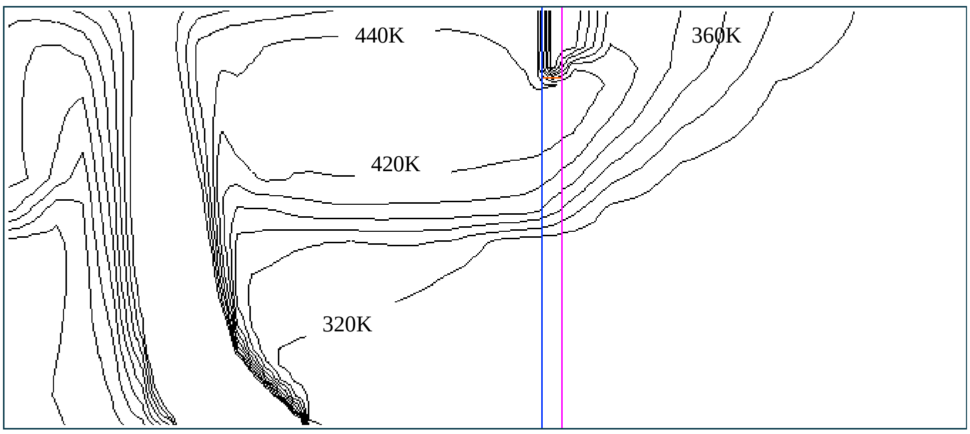

Figure 28 - Temperature contour plot produced by SMARTFIRE using the combustion

Depicted in Figure 26, Figure 27 and Figure 28 are temperature contour plots along the centre of the compartment for PHOENICS, CFX and SMARTFIRE respectively generated using the combustion model. All three SPs depict similar types of behaviour with a similar temperature distribution throughout the compartment. However, the behaviour of the plume appears to be noticeably different in the three cases. The greatest lean towards the rear wall is found in the PHOENICS case followed by the CFX case with SMARTFIRE producing the most up-right plume. This may indicate that more air is being entrained into the PHOENICS plume reducing the overall temperature prediction in the compartment. CFX shows a heating of the floor under the incoming cool air, by radiation from the hot gases.

Comparing the heat source model (Figure 23, Figure 24 and Figure 25) and the combustion model (Figure 26, Figure 27 and Figure 28) it is apparent that the artificial volume created to release the heat source partly defines the nature of the plume. This is most evident on the doorway side of the plume with the cubic nature of the source showing up in all the SPs used in heat source mode. This does not occur in the combustion model. This effect could be minimised by using a volume of reduced height however, this would reduce the volume over which to add the heat increasing the temperature of the flame resulting in too much heat being lost as radiation. This could also lead to problems in convergence. Despite this shortcoming in the heat source model it still produces good agreement with the experimental and combustion model results for the specified monitor locations.

In conclusion, although the SPs display some differences between one another the results are all reasonably close and self-consistent. It should also be noted that these results may be greatly improved using more sophisticated boundary conditions, grid refinement and other physical models that have not been used in the phase-1 exercise.

3.2.2 2000-2-3 – Open Fire with Lid case

This test is an artificial fire test case. There are no experimental results for comparison purposes. Its primary purpose is to test the fire models predictive capability in predicting temperature and flow distributions in a small well ventilated compartment subjected to a non-spreading fire. Predictions of several parameters are made and cross compared.

This fire case utilises a volumetric heat source. The compartment is completely open apart from a solid ceiling (see Figure 29). The fire is located on the floor at the centre of the building. The prescribed fire volume is 1m x 1m x 1m. The fire power is defined as H = $0.188t^2$(kW) (i.e. t squared fire and t is measured in seconds). The compartment is 5m(wide) $\times$ 5m(long) $\times$ 3m(high). The ceiling is adiabatic. The ambient temperature is 303.75K. The case was run for 110s of simulated time using 110 timesteps of 1s.

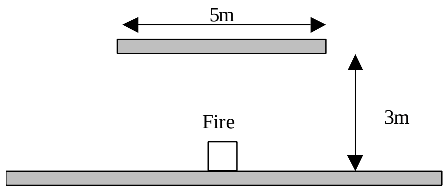

Figure 29 - Configuration of open fire with lid

See Appendix C.3 for further setup details. The PHOENICS and SMARTFIRE simulations make use of the six-flux radiation model while in CFX the discrete transfer model is used with a single ray in the co-ordinate direction to emulate the behaviour of a six-flux radiation model.

All the results below show the temperature distribution at 110 seconds.

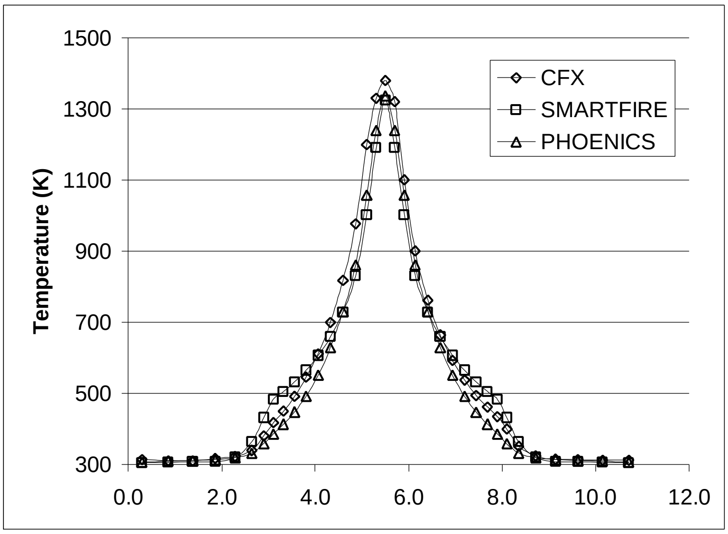

Figure 30 - Temperature profile 0.1m below ceiling along centrally located x - axis

Depicted in Figure 30 is the temperature distribution 0.1m below the ceiling along the centrally located x-axis. As can be seen, all three SP's produce temperature predictions that are in broad agreement. There is a 5% difference in the maximum ceiling temperature predicted. CFX predicts the highest temperature at 1380K while SMARTFIRE predicts the lowest temperature at 1320K. There also appears to be a slight difference in the temperature profile at approximately 0.3m and 0.8m along the ceiling. At these locations, SMARTFIRE appears to predict slightly elevated temperatures. At the same locations, CFX appears to predict a much smaller increase in the temperature, but this is still greater than the temperature predicted by PHOENICS.

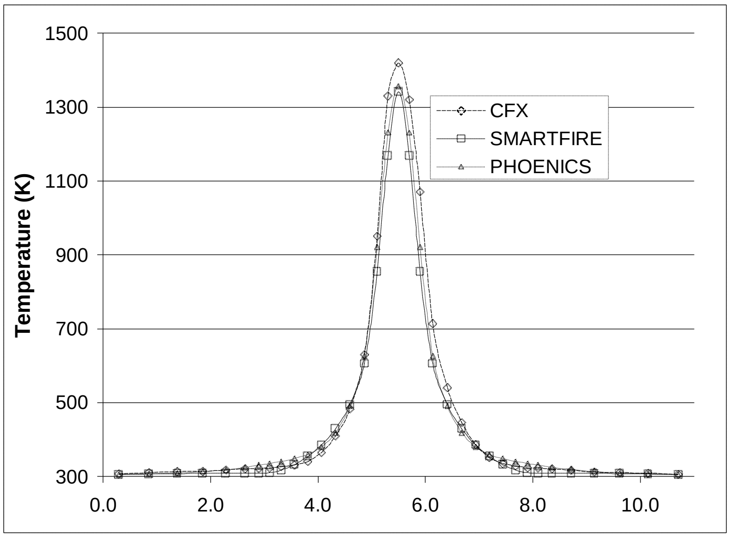

Figure 31 - Temperature profile 0.3m below ceiling along centrally located x - axis

From Figure 31 it can be seen that the temperature profiles of all the SPs are very similar.

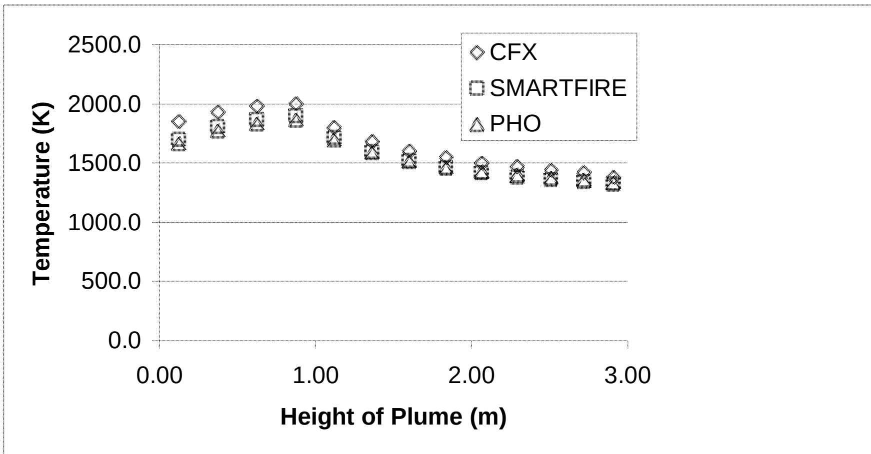

Figure 32 - Temperature profile through the centre of the fire plume

From Figure 32 it can be seen that there is good agreement between the SPs for the predicted plume variation with height.

Depicted in Figure 32 is the variation of plume temperature with height. As can be seen, all three SPs produce the same trends and variation. PHOENICS appears to produce the cooler temperatures with CFX producing the hottest temperatures. The variation between the maximum temperatures is shown in Table 3. As can be seen there are no significant differences in the predicted peak temperatures.

Table 3 - Variation of peak temperature between SPs for 2000-2-3

	PHOENICS	SMARTFIRE	CFX
Maximum Temp	**1860K**	**1900K**	**2000K**
%difference with PHOENICS	**-**	**2.15%**	**7.53%**

Depicted in Figure 33, Figure 34 and Figure 35 are the temperature contours through the vertical central plane passing through the fire plume as predicted by CFX, PHOENICS and SMARTFIRE respectively. The temperature contours are separated by 200 degrees and range between 400K to 1600K. From these figures it is apparent that SMARTFIRE, PHOENICS and CFX produce similar profiles that resemble a fire plume impacting on a flat ceiling.

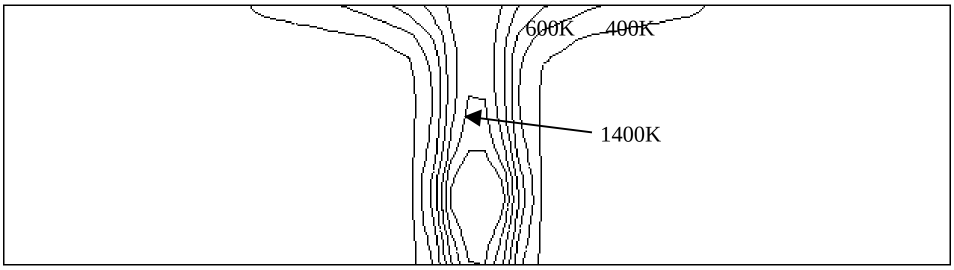

Figure 33 – CFX generated temperature contours through plume on central vertical plane

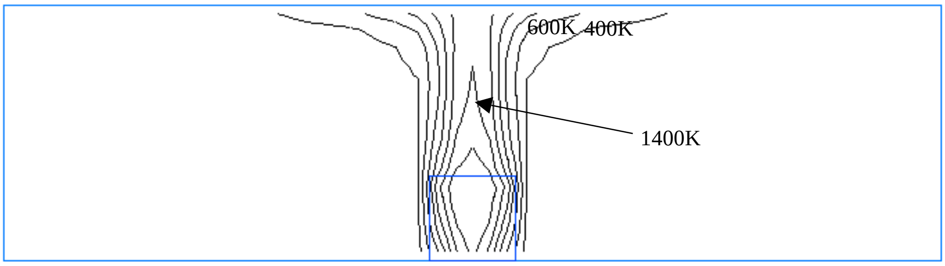

Figure 34 – PHOENICS generated temperature contours through plume on central vertical plane

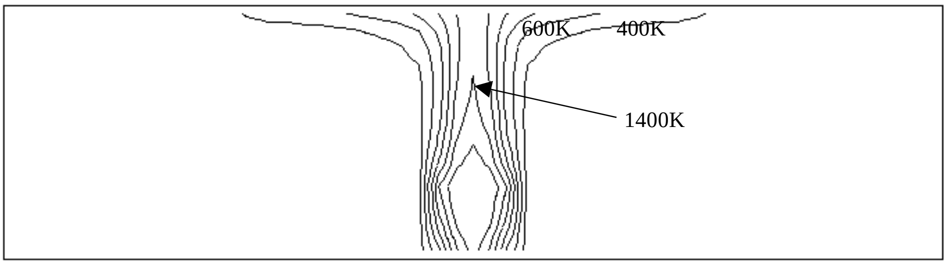

Figure 35 – SMARTFIRE generated temperature contours through plume on central vertical plane

3.2.3 2000-2-4 – CIB W14 case

This case arises from the CIB round robin tests of which subscenario B1 is the case of interest [8]. The fire compartment measured 14.4 m × 7.2 m in plan and 3.53 m in height and contained a doorway of dimensions 2.97 m × 2.13 m. The walls of the compartment were made of aerated concrete blocks (with siporex mortar) with thickness 0.3 m and the following material properties: specific heat 1.05 kJ/kg.K, thermal conductivity 0.12 W/m.K and density 500 kg/m^3. The initial air temperature was measured as 20.0 ^{o}C.

The fire was located on the floor in the centre of the room. The fire fuel consisted of softwood (Pinea ecelsa) timber cribs nailed into 40mm x 40mm battens. The crib measured 2.4m in length, 2.4 m in width and 1.4 m in height.

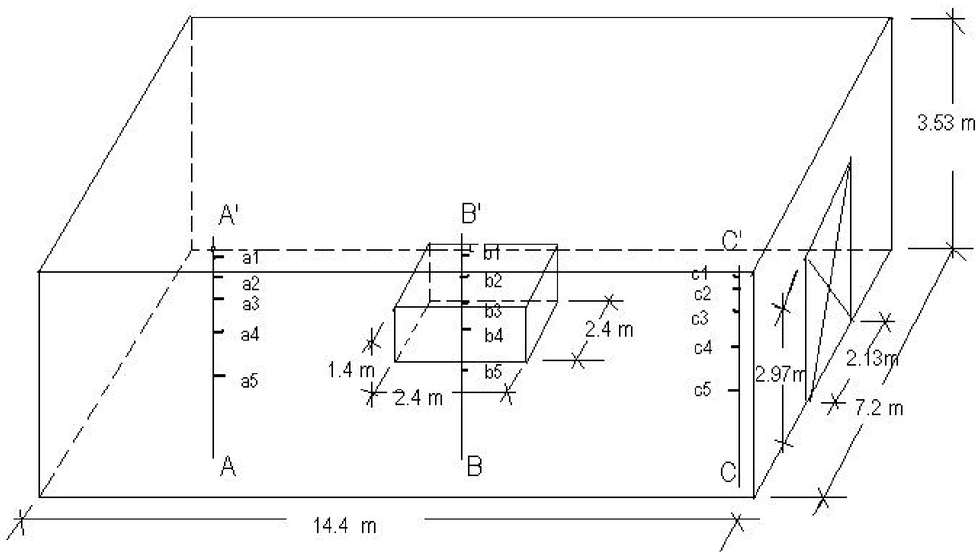

Figure 36 – Depiction of fire compartment geometry showing location of fire source.

The heat release rate ($\dot{Q}$) is given by the following calculation: -

$$\dot{Q} = c \cdot \Delta H_c \cdot \dot{m}$$

The efficiency factor (c) and heat of combustion (ΔH_c) were given as c =0.7 and ΔH_c is 17.8 MJ/kg for burning wood with a 10% moisture content and the mass loss rate ($\dot{m}$) (kg/s) for the wood crib is presented in the table below. A maximum heat release rate of approximately 11 MW was produced. It is assumed that the fuel molecule is $CH_{1.7}O_{0.83}$.

Time (s)	0	60	120	180	240	300	360	420	480	540	600
Mass loss rate(kg/s)	0	0.005	0.004	0.009	0.013	0.014	0.019	0.033	0.052	0.08	0.207

The case was run assuming that all the walls were adiabatic and were completely reflecting (emissivity = 0.0). The case was run for 600s of simulated time using 120 timesteps of 5s.

See Appendix C.4 for further setup details

Comparisions between predicted and measured temperatures at termocouple stacks A, B and C are illustrated in Figure 37 - Figure 44. The locations of the thermocouple can be seen in Figure 36.

It can be seen that in all cases the temperature is overestimated by all the CFD codes. It should be noted that the differences may be due to errors in the experimentally determined mass loss rate. Cross comparing the SPs we note that all are in reasonable agreement with one another. Generally CFX produces the hottest results and PHOENICS the coolest.

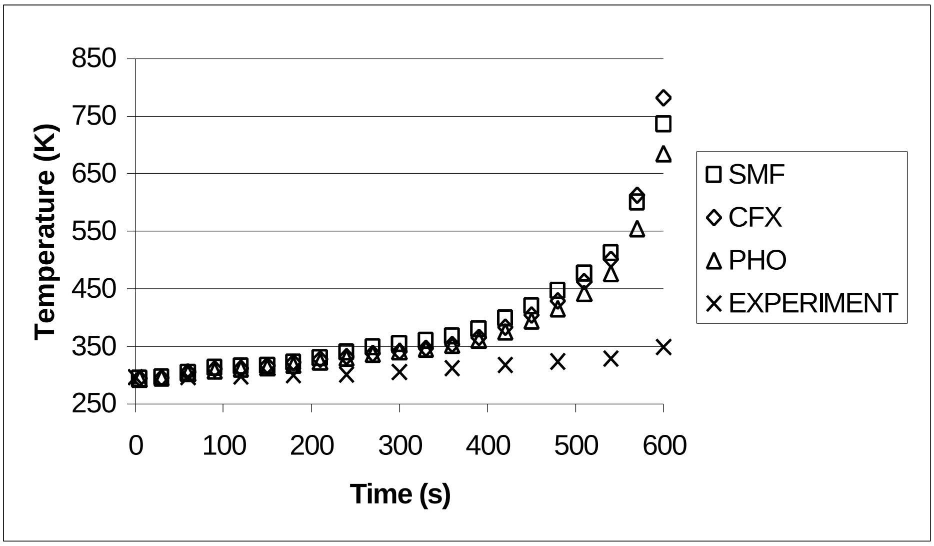

Figure 37 – Temperature history for Ta(1)

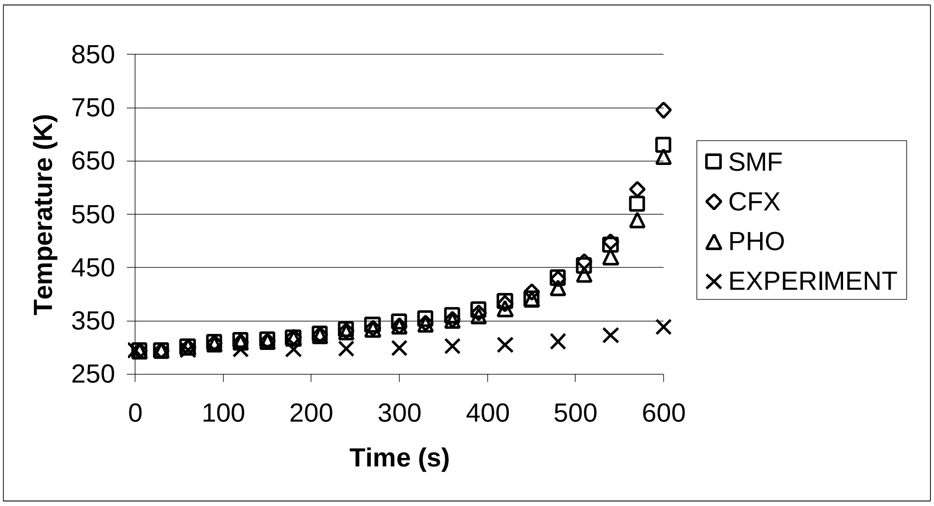

Figure 38 - Temperature history for Ta(3)

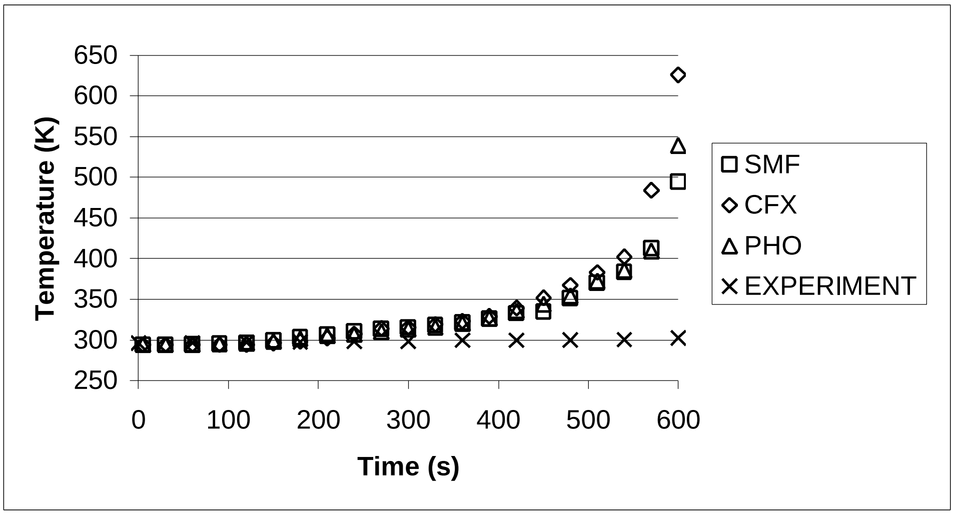

Figure 39 - Temperature history for Ta(5)

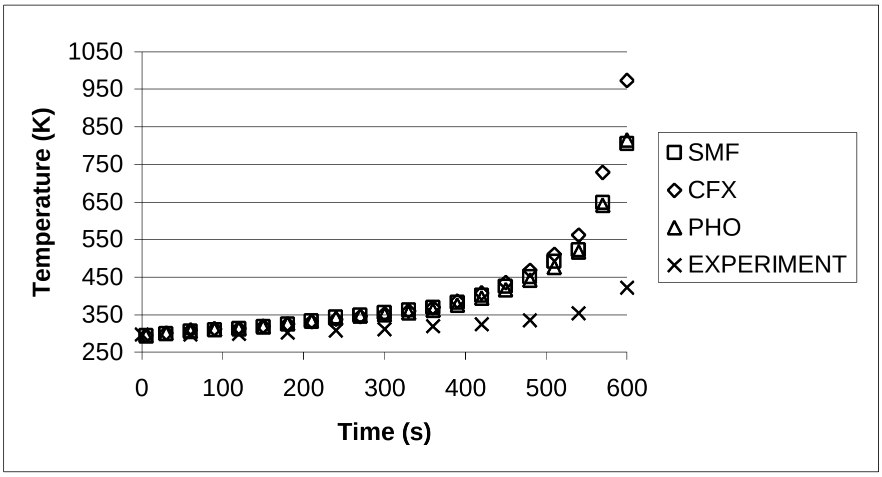

Figure 40 - Temperature history for Tb(1)

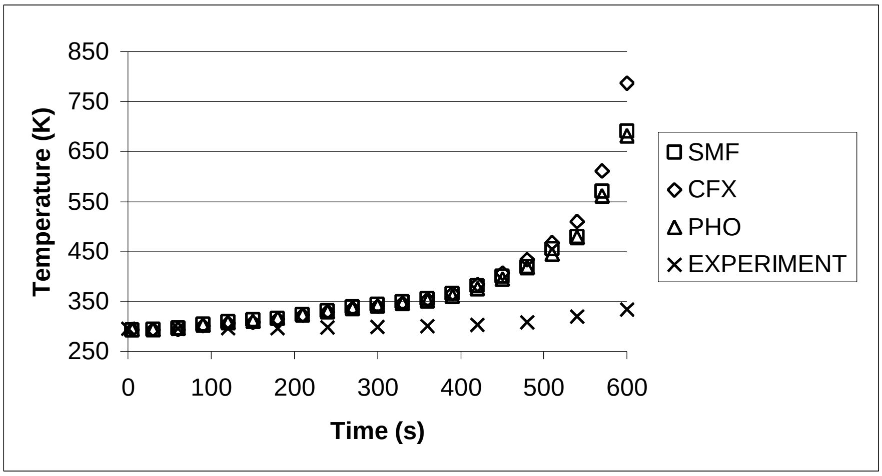

Figure 41 - Temperature history for Tb(3)

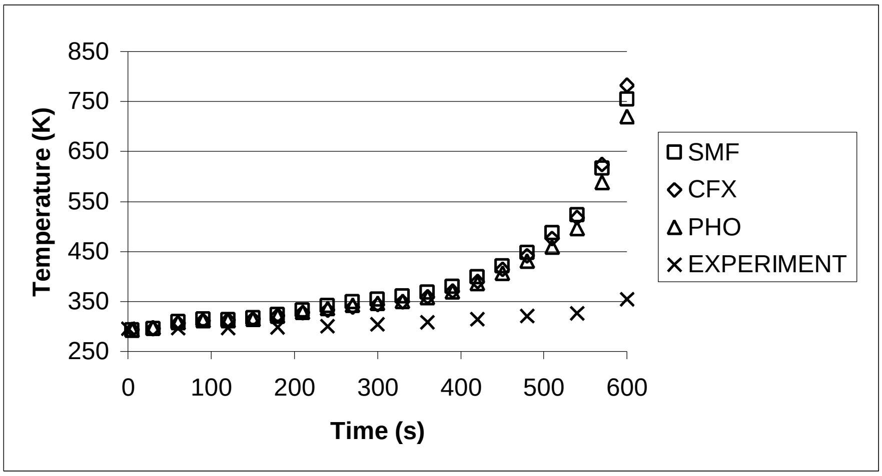

Figure 42 - Temperature history for Tc(1)

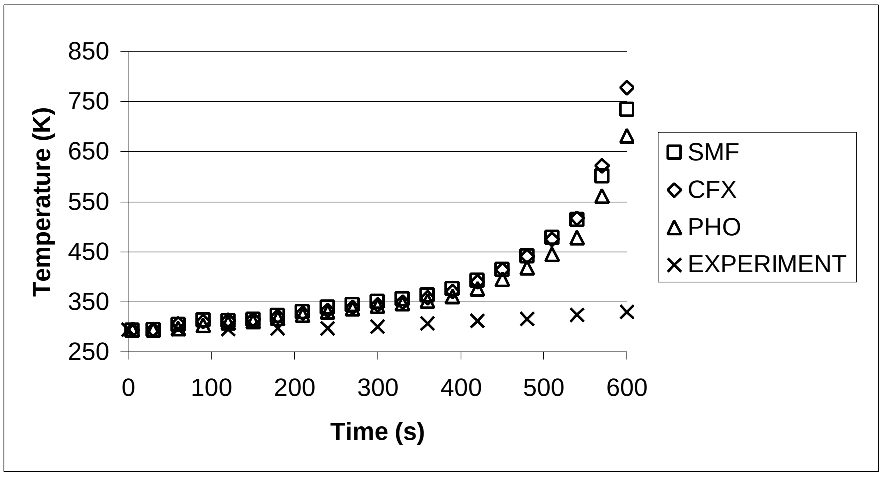

Figure 43 - Temperature history for Tc(3)

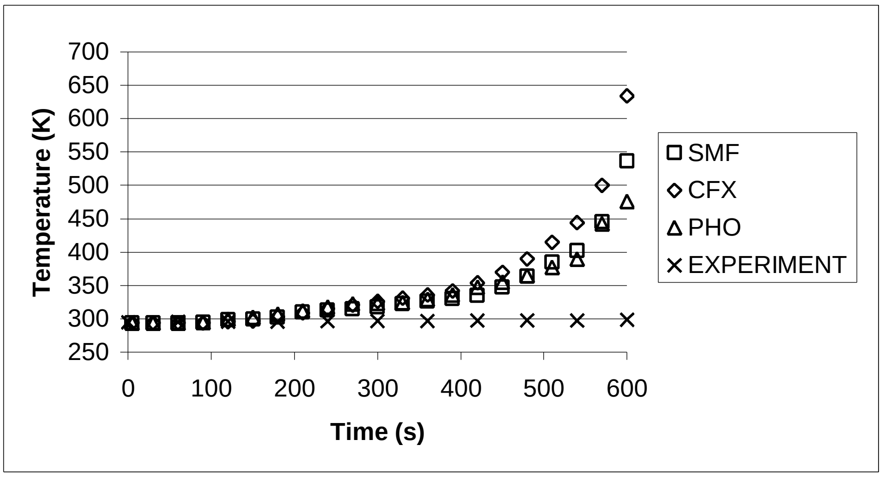

Figure 44 - Temperature history for Tc(5)

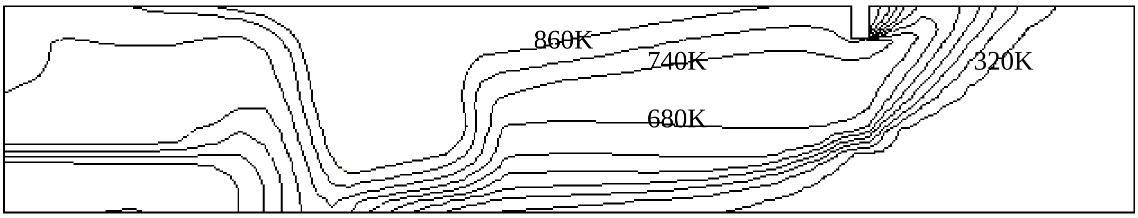

Figure 45 – CFX predicted temperature contour s through the vertical central plane.

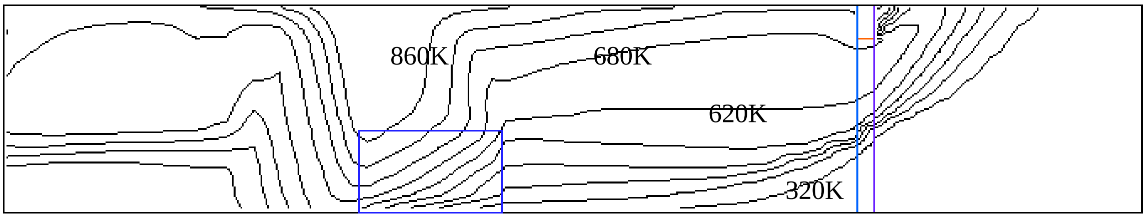

Figure 46 – PHOENICS predicted temperature contour s through the vertical central plane.

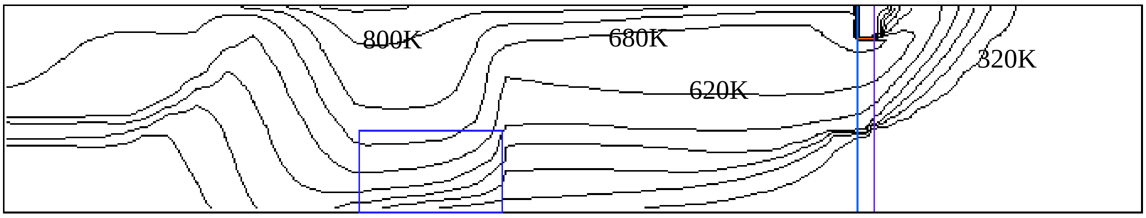

Figure 47 – SMARTFIRE predicted temperature contours through the vertical central plane.

Depicted in Figure 45 to Figure 47 are temperature contours along the centre vertical plane at 600 seconds into the simulation as generated by the three SPs. The temperature contours are separated by 60K and range from 320K to 860K. From these figures it is clear that the variation between the predictions made by the SPs is largest in the near field region above the fire source. In the far field region, temperatures are much closer together, particularly when comparing SMARTFIRE against PHOENICS. CFX produces slightly hotter results which may be due to the use of the non-standard usage of the CFX radiation model with one-ray. It is also expected that the results would be overpredicted due to the use of 1) adiabatic walls and 2) perfectly reflecting walls.

With all the SPs it can be seen that the plume leans away from the doorway.

Due to time constraints it was not possible to run the SPs for a longer simulation time. This would have proved useful as additional experimental data is available for comparison purposes. In addition, it would be interesting to compare the maximum temperatures predicted by the three SPs.

3.2.4 2000-2-5 – LPC007 case

This test case arises from a fire test conducted by the Loss Prevention Council (LPC)[9]. The test is a burning wood crib within an enclosure with a single opening. The test compartment is illustrated below and had a floor area of 6m x 4m and a 3.3m high ceiling. The compartment contained a doorway (vent) measuring 1.0m x 1.8m located on the rear 6m x 3.3m wall. The walls and ceiling of the compartment were made of fire resistant board (Asbestos) which were 0.1m thick. The floor was made of concrete.

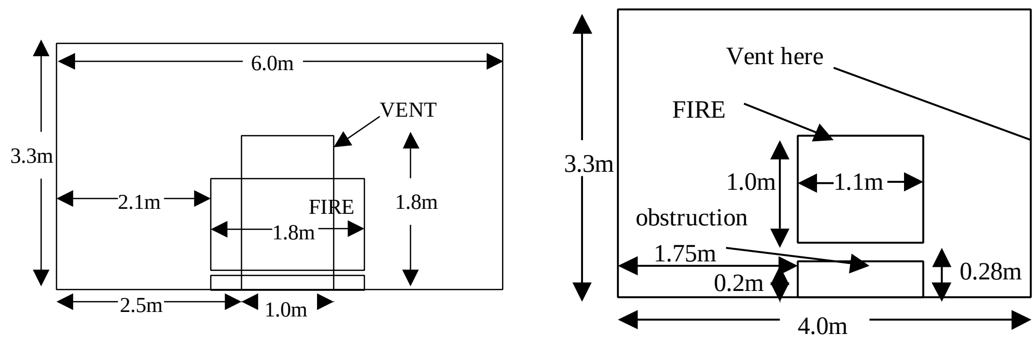

y-z view x-y view

The heat release rate ($\dot{Q}$) is given by the following calculation (see equation 1).

$$\dot{Q} = c \cdot \Delta H_c \cdot \dot{m} \qquad (1)$$

The efficiency factor (c) and heat of combustion (ΔH_c) were given as c =0.7 and ΔH_c is 17.8 MJ/kg for burning wood with a 10% moisture content and the mass loss rate ($\dot{m}$) (kg/s) for the wood crib is presented in Table 4. It is assumed that the fuel molecule is $CH_{1.7}O_{0.83}$.

Table 4: Mass Loss rate for LPC fire test case.

Time(s)	0	150	450	460	1650
$\dot{m}$ (kg/s)	0	0.01835	0.18636	0.1978	0.1978

See Appendix C.5 for further setup details

The results for the plume thermocouple and room corner thermocouple stack for the first 300s are shown in Figure 48 and Figure 49. The lower (L) and higher (H) values refer to measurements at 1.5m and 3.0m above the ground respectively. The corner thermocouple stack is located at 0.57m away form the side wall and 0.5m away from the front wall containing the vent. The plume temperature measurements were taken at 3.0m away from the side wall and 2.392m away form the back wall of the compartment.

This test case proved problematic due to the high temperatures involved and the limited compartment ventilation. From the experimental data, the compartment achieves a flashover between 150 and 450 seconds. Numerically, all the codes were predicting very high temperatures within the first 300 seconds. The temperatures predicted indicate that by 300 seconds the compartment had reached flashover conditions.

After 300 seconds, it was not possible to achieve well-converged solutions for any of the SPs and so all the simulations were terminated at this point. The simplistic and artificial nature of the boundary conditions used in this case are thought to contribute to the premature development of the flashover and the poor convergence characteristics. The walls are treated as adiabatic and radiatively reflective which results in large amounts of heat being retained within the compartment.

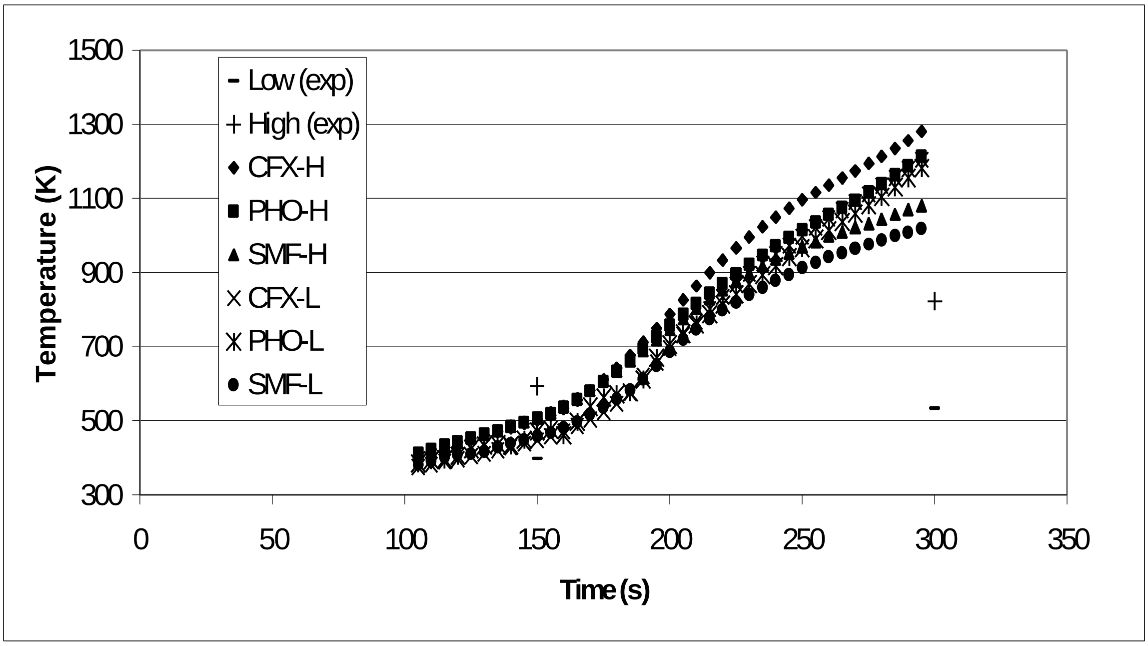

Figure 48: Predicted and measured Corner Stack Temperatures at 1.5m (L) and 3.0m (H) above the floor for the LPC test case.

Up to approximately 200 seconds there is good agreement between all the SPs for both the corner stack and plume predictions. At 150 seconds, the SPs appear to under predict the higher temperatures and over predict the lower temperatures. The predicted level of stratification thus appears to be less than that suggested by the experimental results.

After approximately 200 seconds differences between the predictions generated by the various SPs begin to appear and all of the SPs tend to seriously over predict the experimental results. The plume temperatures are difficult to assess as the movement of the plume can have a significant effect on the value whether experimental or predicted. One consistent feature produced by the SPs is that the lower predicted temperature is consistently hotter than the upper predicted temperature. This trend was not observed in the experimental results. One difference between the experimental setup and the simulations is that the burning wooden crib would cause an obstruction to the flow which is not modelled and may cause significant differences in the near field region of the fire. With all the SPs the hottest temperatures are at the lower point as the hot gases cool as they leave the plume. In the experiment it is possible that the combustion process is occurring higher in the compartment which could be attributable to the obstructing effect of the crib on the oxidant flow.

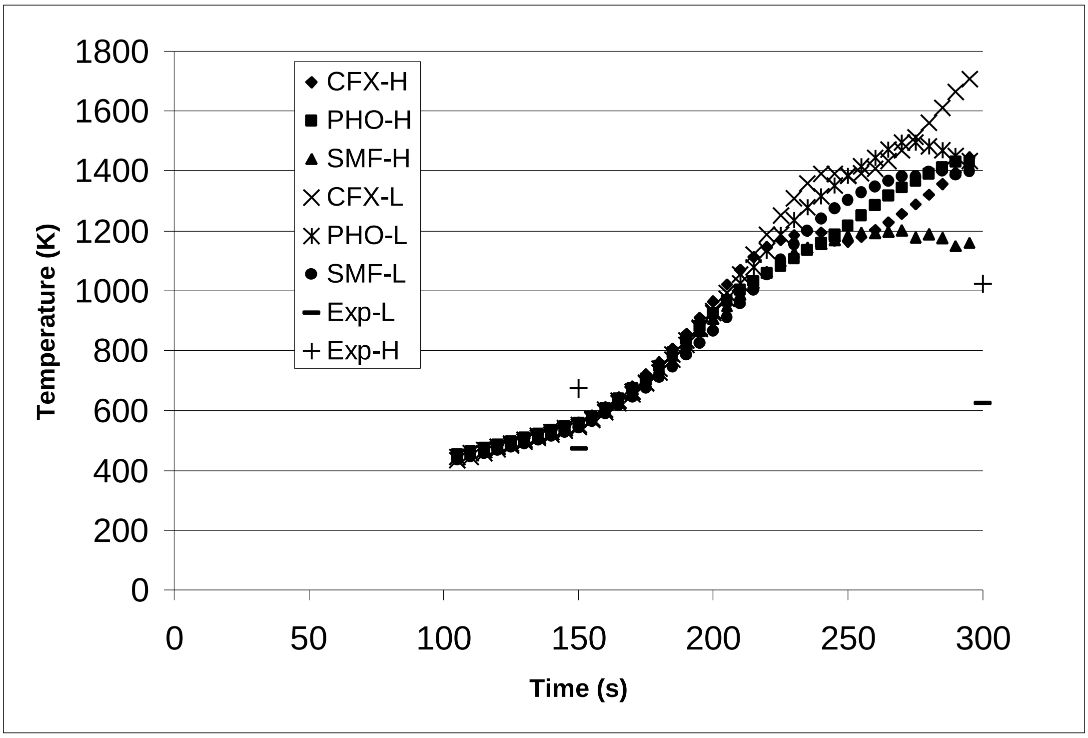

Figure 49: Predicted and measured Plume temperatures at 1.5m (L) and 3.0m (H) above the floor for the LPC test case.

The differences between the observed and predicted results may be due to the artificial nature of the boundary conditions used in this benchmark case. This will be examined further in the Phase 2 analysis.

In the figures below it can be seen that SMARTFIRE (Figure 50) and CFX (Figure 51) produce plumes that lean towards the window. However the PHOENICS (Figure 52) plume leans over to a much lesser degree. From these figures it is clear that the temperature measurement at the lower level for the SPs will be greater than the temperature measurement at the higher level. From these figures it can be further seen that CFX has the hottest plume followed by PHOENICS with SMARTFIRE being the coolest. It is possible that the use of the one-ray radiation model in the CFX simulation has contributed to the higher temperature predicted than might be otherwise expected.

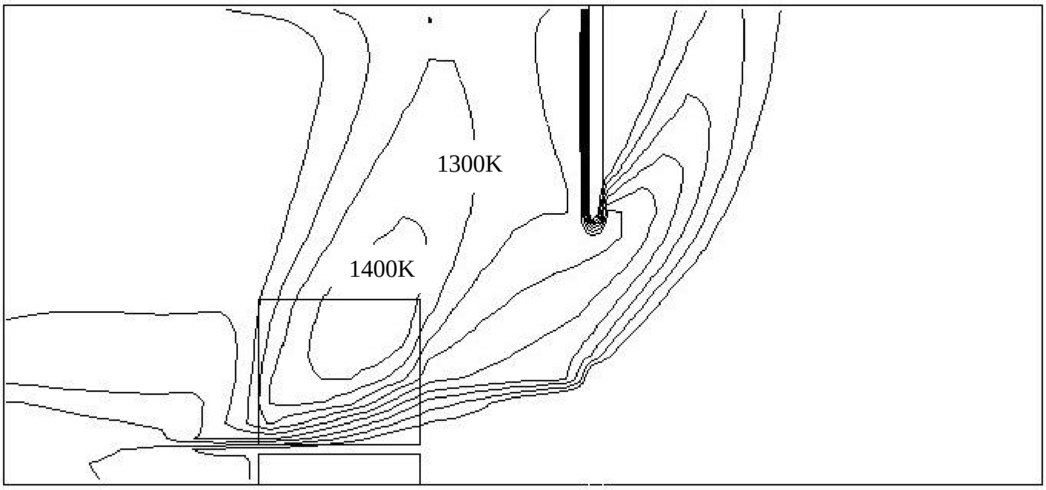

Figure 50 - SMARTFIRE plume at 300s

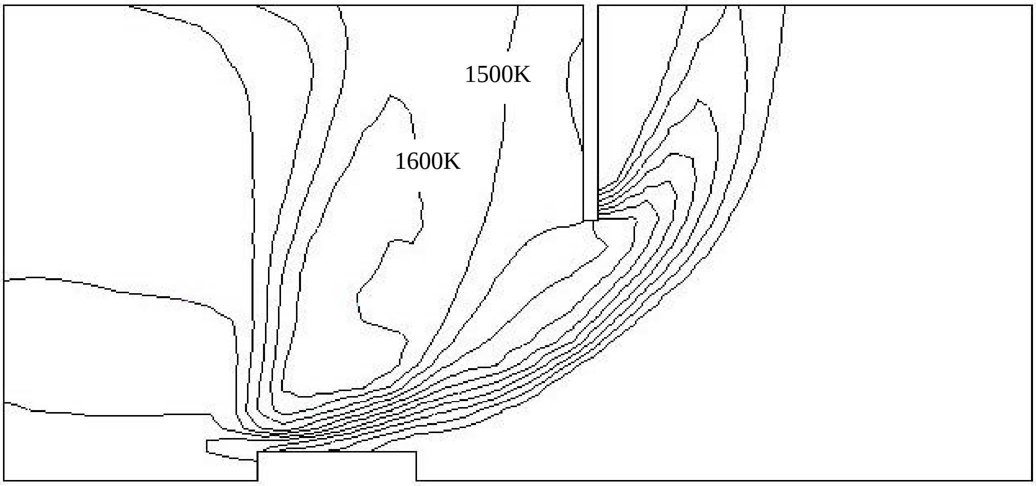

Figure 51 - CFX Plume at 300s

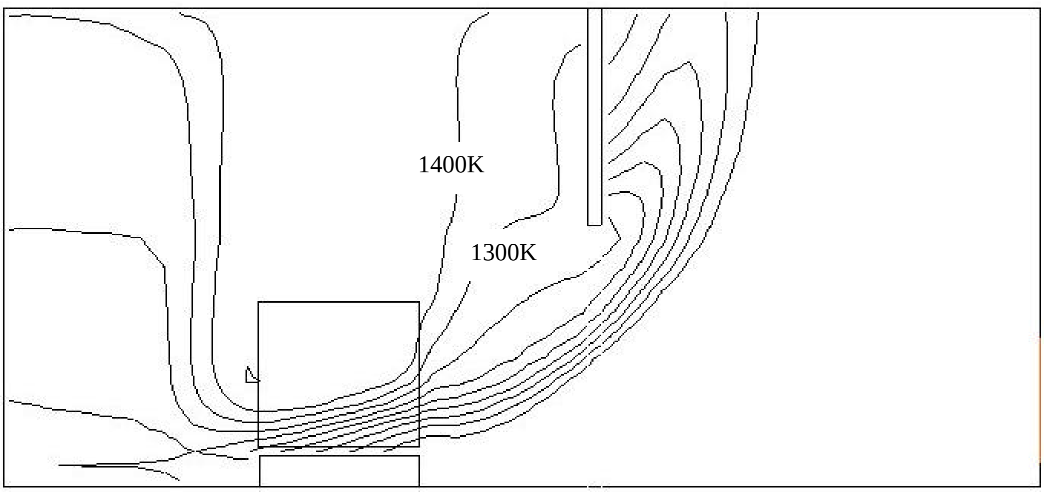

Figure 52 - PHOENICS plume at 300s

4.0 GENERAL DISCUSSION

In studying the outcome of the Phase 1 test cases, it is clear that when identical physics is activated, identical computational meshes used and similar convergence criteria applied, all of the software products tested are capable of generating similar results. This is an important observation and suggests – that within the limitations of the tests undertaken – that these three codes have a similar basic capability and are capable of achieving a similar basic predictive standard.

The results from the CFD test cases are consistent with the view that the basic underlying physics implemented within the codes are similar and are capable of producing similar representations of the physical phenomena modelled. In addition, where experimental results or theoretical solutions are available, the software products have produced reasonable agreement with these results. No doubt, it could be argued that improved agreement could be achieved if the spatial mesh and time stepping are improved. This may be demonstrated in the Phase 2 simulations.

The one area that showed relatively poor agreement with theoretical results concerned the radiation model performance. The six-flux radiation model used by SMARTFIRE and PHOENICS produced very similar results however, they displayed significant differences to the theoretical results. While the six-flux model appears capable of representing the average trends within the compartment, it does not produce an accurate representation of local conditions. The CFX radiation model when used with a single ray (the closest approximation to the six-flux model possible but not mathematically equivalent) displays a more significant weakness and severely under predicts the emissive power in the cavity. It should however be noted that the producers of CFX do not recommend that the discrete transfer radiation model be used with so few rays. The radiation model used by CFX is inherently a more sophisticated model then the six-flux model and is capable of utilising more rays.

It should be recalled that the purpose of the Phase 1 test cases was to compare the performance of the various codes when similar physics capabilities were utilised in all three codes. It should however be noted here that when 12 rays are used in the CFX radiation model, it produces very good agreement with the theoretical results. It is clear from these results that users should be aware of the limitations of the six-flux model when performing fire simulations. Situations that are strongly radiation driven, such as the prediction of flame spread over solid surfaces, or structural response to fire should be treated with care. When using the six-flux model, it is possible that target surfaces would not be preheated by radiation to the extent that would otherwise occur, thereby slowing the flame spread process or unreliably predicting structural response.

The fire cases were intended to provide a more challenging series of tests. Unlike the simple CFD test cases, the fire cases make use of a range of CFD capability. Furthermore, they focus attention on the software's capability within the specific domain of interest i.e. fire modelling.

The first two fire cases consisted of the small non-spreading fire within the small ventilated compartment modelled using heat source and gaseous combustion model. For these cases, all the software products appear to produce a good representation of the measured temperature distribution within the compartment and velocity profile within the doorway. Furthermore, there are insignificant differences between the temperatures predicted by heat source model and gaseous combustion model. However, all the software products appear to slightly over predict the hot layer temperature. This over prediction is likely to be due to the simple specification of the conditions required in phase 1. No doubt, it could be argued that improved agreement could be achieved if more sophisticated physics were used in the simulations. This may be demonstrated in the Phase 2 simulations. It should however be pointed out that the fire in this case is quite small and so radiative heat transfer does not play a significant role in this situation.

The third fire case consisted of a fire – represented by a prescribed heat release rate – centrally located in the open compartment. While there were no experimental results for comparison purposes, it was clear that all three software products produced near identical results.

The forth fire case consisted of a large fire in a medium sized compartment which was well ventilated. The fire was modelled using a prescribed mass release rate in conjunction with a gaseous combustion model. Here again all three software products produced good agreement when compared with each other. However, towards the end of the simulation period, there was a significant difference between the predicted and measured temperatures. This is thought to be due to problems with the experimentally determined heat release rates. Had time permitted, it would have been interesting to continue the numerical predictions for a longer period of time to compare the maximum temperatures produced by the various codes.

The fifth fire case consisted of a large fire in a small sized compartment which was under ventilated. The fire was modelled using a gaseous combustion model. Here again all three software products produced good agreement when compared with each other in the early phases of the fire development. However, towards the end of the simulation period, there was a significant difference between the predicted and measured temperatures and between the predictions produced by the various software products. This is thought to be primarily due to the simplicity of the boundary conditions imposed on the calculations resulting in very high temperatures being generated within the compartment. It is also worth noting that all the simulations had to be prematurely stopped due to convergence difficulties. This test case will be examined further in Phase 2 using more representative boundary conditions.

The results from the fire cases support the conclusions drawn from the CFD test cases. While there are minor differences between the results produced by each of the software products; on the whole they produce – for practical engineering considerations – identical results.

The completion of Phase 1 has highlighted several areas in which improvements can be made to both the procedures used and the test cases examined.

It is suggested that once the test case has been specified at a high level by the BTG, the test case input files should be set up by each of the participating SP developers. These should then be checked by the BTG to ensure that they conform to the standards of the benchmark. In this way, the test case input files would be optimised for the particular SP within the guidelines set down by the BTG. While the representatives of the BTG that conducted the assessments (i.e. FSEG) may have expertise in all of the SPs utilised in this study, it is unlikely that they will have sufficient expertise in all of the products likely to be tested. While this places pressure on the participating software producer to generate the input files, if the benchmarking procedure becomes a recognised standard, code vendors will be prepared to participate at this level.

In addition, once a version of a SP is entered into the benchmarking process, all the test cases must be run with that version. If another release version of the SP is produced, this to will need to go through the benchmark process in its entirety. However, a mix and match process in which different versions of a code are used in order to improve the level of agreement should not be permitted.

With regard to the benchmark cases utilised in the current procedure, several improvements can be suggested for the fire cases.

Fire case 2000-2-4 was run for 10 minutes of simulation time. Although all the SPs exhibit the same growing trend and similar temperatures it would be useful to run the case for a longer time period. This could be compared with the experimental results in order to determine the differences between maximum predicted and maximum measured temperatures.

Fire case 2000-2-5 proved difficult to obtain converged predictions due to the artificial nature of the boundary conditions utilised in Phase 1. This case is also complicated as flashover occurs and the fire becomes ventilation controlled. While it is necessary in Phase 1 to select a set of “simple” boundary conditions that can be represented by most SPs, another choice of boundary conditions would be appropriate. It is possible to run this case with a fixed wall temperature with unit emissivity. It must be noted that these boundary conditions are just as unrealistic as the adiabatic boundary conditions used in Phase 1. However, this would have the effect of artificially removing a large amount of heat from the compartment and may allow the simulation to run for longer.

There is also the need for additional cases to further benchmark the SPs. This need must be balanced against the work that would be involved in carrying out these exercises. One possible candidate case by Isaksson et al[10] gives experimental data and simulation data from JASMINE and SOFIE for a fire in a room with a perforated suspended ceiling. Another possible source of good experimental data concerns a room fire trial conducted by Neilson[11].

5.0 CONCLUDING COMMENTS

The first phase of the testing programme has been successfully completed. In studying the results generated in Phase 1 it is important to note the following points:

1) The results generated and comments made only refer to the software actually used in the trials. This should not simply be taken to mean the product name but also the release number and version number of the software.
2) The Phase 1 results are not intended to represent mesh independent solutions. They are intended to represent converged solutions on "reasonable" meshes. In each test case, the same computational mesh is used by each software product. Phase 2 simulations can be used to explore simulations performed using finer meshes.
3) The Phase 1 results do not make use of the most sophisticated physics available in each of the software products. A base line set of characteristics has been set that allow a fair comparison between the codes. Where model predictions are compared with experimental data, these predictions can be improved through the use of more sophisticated physical sub-models. Phase 2 simulations can be used to explore the benefits of using more sophisticated physics.
4) The series of trials undertaken in this project should not be considered to be definitive. They have been selected as a basis for exploring the potential of the benchmarking process. It is intended that additional tests should be added to the suite of test cases.

In studying the outcome of the Phase 1 test cases, it is clear that when identical physics is activated, identical computational meshes used and similar convergence criteria applied, all of the software products tested are capable of generating similar results. This is an important observation and suggests – that within the limitations of the tests undertaken – that these three codes have a similar basic capability and are capable of achieving a similar basic standard.

The one area that showed relatively poor agreement with theoretical results concerned the radiation model performance. The six-flux radiation model while capable of representing the average trends within the compartment, does not produce an accurate representation of local conditions. It is clear from these results that users should be aware of the limitations of the six-flux model when performing fire simulations. Situations that are strongly radiation driven, such as the prediction of flame spread over solid surfaces and structural response to fire should be treated with care. When using the six-flux model, it is possible that target fuel surfaces would not be preheated by radiation to the extent that would otherwise occur, thereby slowing the flame spread process.

The results from the CFD test cases are consistent with the view that the basic underlying physics implemented within the codes are similar and provide a good representation of reality. This should come as no surprise as all three software products purport to model fluid dynamics processes using similar techniques. However, from a regulatory viewpoint, it is reassuring to have an independent verification of this similarity. In addition, where experimental results or theoretical solutions are available, the software products have produced reasonable agreement with these results. No doubt, it could be argued that improved agreement could be achieved if the spatial mesh and time stepping are improved. This may be demonstrated in the Phase 2 simulations.

The results from the fire cases support the conclusions drawn from the CFD test cases. While there are minor differences between the results produced by each of the software products; on the whole they produce – for practical engineering considerations – identical results.

A significant – and somewhat reassuring - conclusion to draw from these results is that an engineer using the basic capabilities of any of the three software products tested would be likely to draw the same conclusions from the results generated irrespective of which product was used. From a regulators view, this is an important result as it suggests that the quality of the predictions produced are likely to be independent of the tool used – at least in situations where the basic capabilities of the software are used.

A second significant conclusion is that within the limits of the test cases examined and taking into consideration experimental inconsistencies and errors, all three software products are capable of producing reasonable engineering approximations to the experimental data, both for the simple CFD and fire cases.

What remains to be completed at this stage are the Phase 2 results produced by the other testers. In Phase 2, the modellers are free to select which of the test cases to repeat using the full capability of their software. These results will then be checked by FSEG for their veracity.

Finally, the concept of the Phase 1 testing protocols has been shown to be a valuable tool in providing a verifiable method of benchmarking and gauging the basic capabilities of CFD based fire models on a level playing field. To further improve the capabilities of the approach, it is recommended that additional test cases in the two categories be developed and several of the fire cases be refined.

References

1. `CFX4, Version 4.2', AEA Technology. Harwell, England.
2. H. I. Rosten, D. B. Spalding and D. G. Tatchell, `PHOENICS: A General-Purpose Program for Fluid-Flow, Heat-Transfer and Chemical-Reaction Processes', in Proceedings of the 3rd International Conference on Engineering Software, 639-655 (1983).
3. Galea E., Knight B., Patel M., Ewer J., Petridis M., and Taylor S., "SMARTFIRE V2.01 build 369D, User Guide and Technical Manual", SMARTFIRE CD and bound manual, 1999
4. C. M. Rhie and W. L. Chow, `Numerical Study of the Turbulent Flow Past an Airfoil with Trailing Edge Separation', AIAA Journal, 21(11), 1525-1532 (1983).
5. J. Kim, S. J. Kline and J. P. Johnston, "Investigation of a Reattachment Turbulent Shear Layer: Flow over a Backward-Facing Step", Transactions of the ASME, Journal of Fluids Engineering, 102, 302-308, 1980
6. R. Cheesewright, K. J. King, and S. Ziai, "Experimental data for the validation of Computer Codes for the prediction of Two-Dimensional Buoyant Cavity Vlows", Significant Questions in Buoyance Affected Enclosure or Cavity Flows, vol. HTD-60, pp 75-81, ASME, New York, 1986
7. Steckler, K.D, Quintiere, J.G and Rinkinen, W.J., "Flow induced by fire in a compartment", NBSIR 82-2520, National Bureau of Standards, 1982.
8. Hostikka S and Keski-Rahkonen O., Results of CIB W14 Round Robin for Code Assessment Scenario B. Draft 31/08/98, VTT Technical Research Centre of Finland.
9. Glocking, J.L.D, Annable, K., Campbell, S.C. "Fire Spread in multi-storey buidings – *'Fire break out from heavyweight unglazed curtain wall system – Run 007'* ", LPC Laboratories rep. TE 88932-43, 25 Feb 1997.
10. Isaksson S., Persson B., and Tuovinen H., "CFD-Simulatons of Fire Detection in a Room with a Perforated Suspended Ceiling, BRANDFORSK Project 628-951", SP Report 1997:43, SP Swedish National Testing and Research Institute, 1997
11. Nielson C., "An Analysis of Pre-Flashover Fire Experiments with Field Modelling Comparisons", Fire Engineering Research Report 2000/10, Department of Civil Engineering, University of Canterbury, New Zealand, March 2000, ISSN 1173-5996